



NIC Symposium 2012

7 – 8 February 2012
Forschungszentrum Jülich, Germany

Programme

Bus Schedule

Poster Abstracts

Participants

Programme

Tuesday, 7 February 2012

- 8.30 Transfer from Jülich
- 8.45 Registration
- 9.00 **Welcome Address** by A. Bachem, Chairman of the Board of Directors,
Forschungszentrum Jülich
- 9.15 Th. Lippert, Forschungszentrum Jülich
Supercomputing at Scale
- 10.00 K. Binder, Universität Mainz
25 years HLRZ/NIC: Taking the Lead in Supercomputing in Germany
- 10.30 Coffee
- 11.00 A. Groß, Universität Ulm
Ab initio Molecular Dynamics Simulations of Molecule-Surface Interactions
- 11.45 W. Paul, Universität Halle
**Structure and Dynamics at Polymer-Solid Interfaces: A Molecular Dynamics
Simulation of 1,4-Polybutadiene on Graphite**
- 12.30 Lunch
- 14.00 K. Rushchanskii, Forschungszentrum Jülich
Computational Studies of Insulating Magnetic Oxides
- 14.45 A. Muramatsu, Universität Stuttgart
Quantum Spin Liquid in Correlated Fermions on a Graphene-Like Structure
- 15.30 Coffee
- 16.00 N. Atodiresei, Forschungszentrum Jülich
**Understanding Molecular Electronics and Spintronics from First Principles
Simulations**
- 16.45 B. Gmeiner, Universität Erlangen
Highly Parallel Geometric Multigrid Algorithm for Hierarchical Hybrid Grids
- 17.30 Poster Session and Reception
- 19.00 Transfer to Jülich

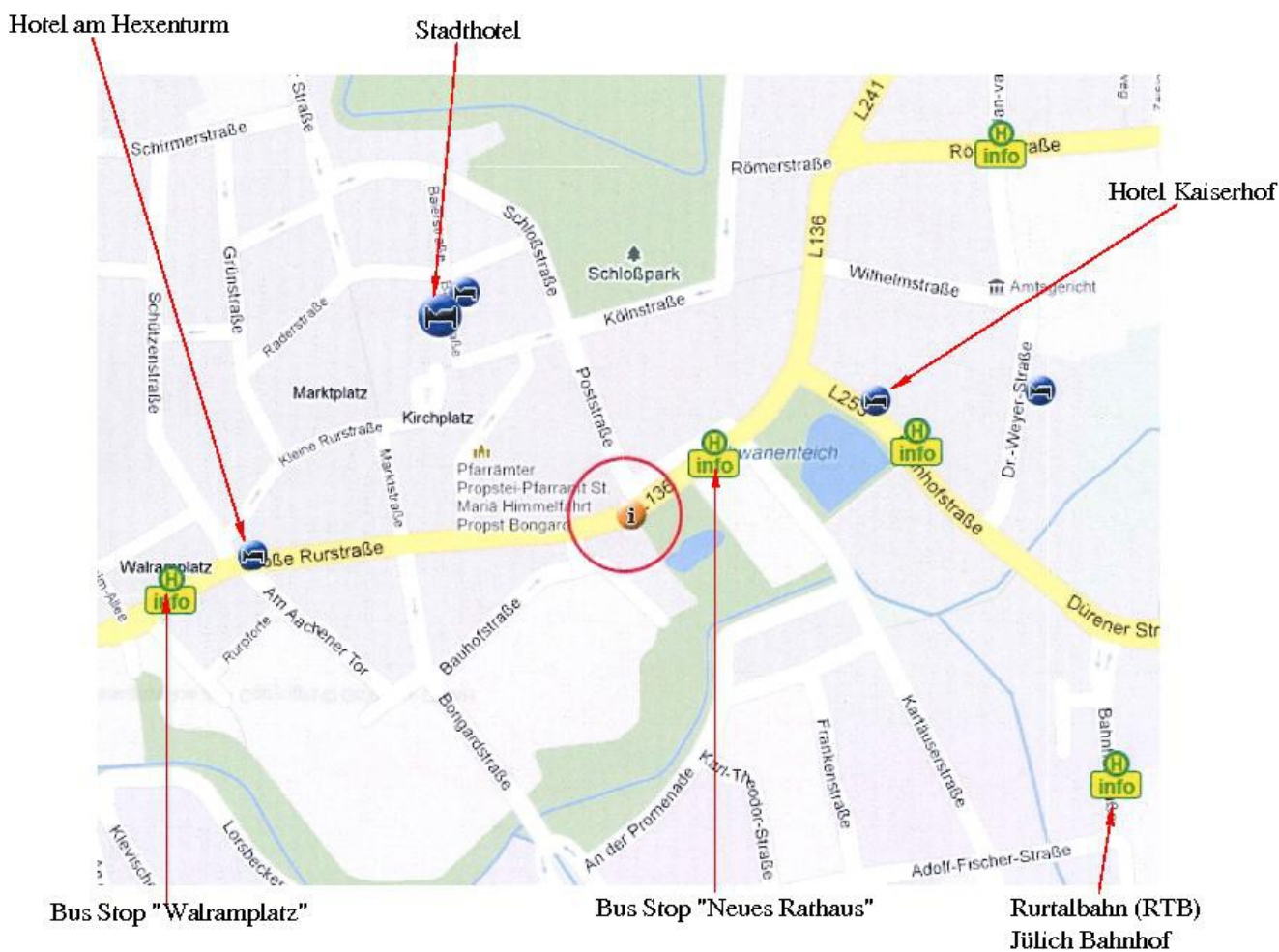
Wednesday, 8 February 2012

- 8.30 Transfer from Jülich
- 9.00 D. A. Fedosov, Forschungszentrum Jülich
Mesoscale Simulations of Human Blood Flow: From Red Blood Cell Elasticity and Interactions to Blood Rheology
- 9.45 J. Harting, Universität Stuttgart
Colloidal Particles at Liquid Interfaces: From Bijels to Pickering Emulsions
- 10.30 Coffee
- 11.00 U.-G. Meißner, Universität Bonn
Nuclear Physics from Lattice Simulations
- 11.45 H. Wittig, Universität Mainz
Probing the $N_f = 2$ QCD Phase Transition with Light Wilson Fermions
- 12.30 Lunch
- 14.00 R. Banerjee, Universität Hamburg
Generation of Strong Magnetic Fields via the Small-Scale Dynamo from Gravity Driven Turbulence
- 14.45 J. P. Mellado, MPI für Meteorologie
Direct Numerical Simulation of Turbulent Mixing in the Planetary Boundary Layer
- 15.30 Coffee
- 16.00 D. Bauer, Universität Rostock
Study of Plasma Formation and Ionization Dynamics in Intense Laser Fields by Means of Massively Parallel Particle-in-Cell Simulations
- 16.45 G. Geiser, RWTH Aachen
A Hybrid Aeroacoustic Prediction Method for Non-Reactive and Reactive Flows
- 17.45 Transfer to Jülich and to Düren Train Station

Bus Schedule

Bus is free of charge for participants.

Date	Departure Time	Meeting Point	Destination
7 February	08:30	Bus stop "Walramplatz"	Research Centre Jülich, Auditorium
	08:35	Bus stop "Neues Rathaus"	
	19:00	Research Centre Jülich, Auditorium	Hotels in Jülich
8 February	08:30	Bus stop "Walramplatz"	Research Centre Jülich, Auditorium
	08:35	Bus stop "Neues Rathaus"	
	17:45	Research Centre Jülich, Auditorium	Hotels in Jülich Düren Train Station



Poster Abstracts

The number in brackets in front of the title is the number of the movable wall where to place the poster for the poster session.

Elementary Particle Physics

[1] Testing the Standard Model with kaon physics from lattice QCD

A. Juttner, P. A. Boyle, J. M. Flynn, C. T. Sachrajda, K. Sivalingam, J. Zanotti

Our project focuses on evaluating the form-factor at zero momentum transfer for the semileptonic decay of a kaon to a pion plus a lepton and its associated neutrino. Combining this quantity with experimental decay-rate measurements allows the Standard Model parameter V_{us} to be extracted. V_{us} gives the strength of the coupling for a strange quark to decay to a light up quark and is one element of a matrix, known as the Cabibbo-Kobayashi-Maskawa matrix, which is unitary in the Standard Model. A precision determination of V_{us} enables a sensitive test of unitarity of the CKM matrix, failure of which would be a signal of new physics.

With our Jugene allocation we are concentrating on calculating the form factor with simulated pion masses much closer to the physical value. This will greatly improve the accuracy of the so-called chiral extrapolation in mass used to extract the final physical result. It will allow us to go from our existing precision of 0.6% for the form factor to 0.3%, matching improvements in experiment and increasing the power of the CKM unitarity test.

We are calculating quantum mechanical transition amplitudes by Markov chain Monte Carlo methods. The core of the numerical calculations is the solution of extremely large sparse linear systems using Krylov subspace techniques. Careful choice of the input vectors for these systems reduces the computational cost overall, allowing us to reduce statistical errors in tandem with the systematic improvement from simulating at smaller masses.

[2] Baryon octet strangeness content from the lattice

St. Dürr

A report is given for the joint project of the Budapest-Marseille-Wuppertal collaboration and the Regensburg group to study the quark mass-dependence of octet baryons in SU(3) Baryon Chiral Perturbation Theory (XPT). This formulation is expected to extend to larger quark masses than Heavy-Baryon XPT. Its applicability is tested with 2+1 flavour data which cover three lattice spacings and pion masses down to about 190 MeV, in large volumes. We determine both the light and the strange sigma terms for all members of the baryon octet with fully controlled systematics.

[3] Charmed hadron spectroscopy for $N_f=1$

G. Bali, S. Collins, St. Dürr, Z. Fodor, R. Horsley, C. Hoelbling, S.D. Katz, I. Kanamori, S. Krieg, T. Kurth L. Lellouch, T. Lippert, C. McNeile, Y. Nakamura, D. Pleiter, P. Pérez-Rubio, P. Rakow, A. Schafer, G. Schierholz K.K. Szabo, F. Winter, J. Zanotti

Quantum Chromodynamics (QCD) is the theory that describes the strong interactions, i.e., the interactions between quarks and gluons. One important property of QCD is confinement:

Quarks are not observed in isolation but are bound together in mesons (as quark-antiquark pairs) and baryons (which contain three quarks).

The spectroscopy of hadrons containing charm quarks has undergone a renaissance in recent years. The triggering point was the discovery of several new narrow charmonium resonances close to the $D\bar{D}$ thresholds and new narrow D_s mesons close to the DK thresholds. More results are expected to appear in the next few years from currently running experiments, e.g. Belle, BES-III and LHC and the future PANDA experiment at the FAIR facility at the GSI. In this work we study the spectra of charmonium and charm-light mesons, including higher spin states using Lattice QCD.

[4] Precision computation of the kaon bag parameter

S. Dürr, Z. Fodor, C. Hoelbling, S.D. Katz, S. Krieg, T. Kurth, L. Lellouch, T. Lippert, C. McNeile, A. Portelli, K.K. Szabó

Indirect CP violation in $K \rightarrow \pi\pi$ decays plays a central role in constraining the flavour structure of the Standard Model (SM) and in the search for new physics. For many years the leading uncertainty in the SM prediction of this phenomenon was the one associated with the nonperturbative strong interaction dynamics in this process. Here we present a fully controlled lattice QCD calculation of these effects, which are described by the neutral kaon mixing parameter B_K . We use a two step HEX smeared clover-improved Wilson action, with four lattice spacings from $a \approx 0.054$ fm to $a \approx 0.093$ fm and pion masses at and even below the physical value. Nonperturbative renormalization is performed in the RI-MOM scheme, where we find that operator mixing induced by chiral symmetry breaking is very small. Using fully nonperturbative continuum running, we obtain our main result $B_K^{\text{RI}}(3.5 \text{ GeV}) = 0.531(6)_{\text{stat}}(2)_{\text{sys}}$. A perturbative 2-loop conversion yields $B_K^{\text{MS-NDR}}(2 \text{ GeV}) = 0.564(6)_{\text{stat}}(3)_{\text{sys}}(6)_{\text{PT}}$ and $B_K = 0.773(8)_{\text{stat}}(3)_{\text{sys}}(8)_{\text{PT}}$, which is in good agreement with current results from fits to experimental data.

[5] Finite temperature lattice QCD with Wilson quarks

Borsanyi, Hoelbling, Fodor, Katz, Krieg, Nogradi, Toth, K. Szabo, Trombitas

QCD is investigated at finite temperature using Wilson fermions in the fixed scale approach. We use four lattice spacings to allow control over discretization errors. The light quark masses are fixed to heavier than physical values. The renormalized chiral condensate, quark number susceptibility and the Polyakov loop are measured and the results are compared with those of the staggered formulation.

[6] Nucleon distribution amplitudes from lattice QCD

R. Schiel, Bali, Braun, Collins, Göckeler, Hagen, Horsley, Nakamura, Pleiter, Rakow, Schäfer, Schierholz, Stüben, Wein, Zanotti

Understanding the nucleon structure in terms of quarks and gluons presents one of the central goals of the theory of strong interactions. The full nucleon wave function is very complicated and remains elusive so that progress in the theory has mainly been in establishing the areas where QCD predictions only require limited non-perturbative input. In particular, hard exclusive reactions involving large momentum transfer from a point-like source to the final state baryon are mostly sensitive to the wave functions at small transverse separations between the constituents, usually called distribution amplitudes. The normalization constant and the first two moments of the distribution amplitudes can be

calculated non-perturbatively using lattice QCD. Here, we describe an ongoing project by the QCDSF collaboration to calculate distribution amplitudes of the nucleon and its parity partner, $N^*(1535)$. The calculations are done using two flavors of dynamical (clover) fermions on lattices of different volume and pion masses down to 180 MeV.

Astrophysics

[7] Explosion models of core-collapse supernovae

F. Hanke, B. Müller, A. Marek, L. Hudepohl and H.-Th. Janka

Supernova explosions are among the most powerful cosmic events, whose physical mechanism and consequences are still incompletely understood. In this poster we will present our current progress in performing simulations of the neutrino-driven explosion mechanism of core-collapse supernovae. Thereby, we focus on results of three-dimensional calculations with simple neutrino heating and cooling terms running on the JUROPA at NIC that shed light on the controversial question whether and how 3D effects influence the neutrino heating efficiency and thus, whether they influence the neutrino-driven explosion mechanism.

[8] Evolution towards the field binary population in dense star clusters

Th. Kaczmarek, C. Hövel, S. Pfallner

Surveys of the binary populations in the solar neighbourhood have shown, that the periods of G- and M-type stars are *log-normally* distributed in the range from 0.1 days to 10^{11} days. However, observations of young binary populations in various star forming regions suggest a *log-uniform* period distribution rather than a log-normal distribution.

In the here presented study, we investigate, if the early evolution of the binary populations in their natal environments can change an initially log-uniform period distribution to a log-normal one. Most stars, including binaries, form in star clusters of thousands of stars which are embedded in the gas, they are forming from. In these dense systems two important processes take place: i) the orbital decay of embedded binary systems and ii) the destruction of soft binaries in three body interactions.

To investigate the effect of these two processes on the period distribution, we performed Monte-Carlo simulations of binary populations to model the former process, while the latter was simulated using Nbody simulations of a binary population embedded in a ONC-like star cluster. Neither of the two processes is capable to change a log-uniform to a log-normal period distribution. While the orbital decay significantly reduces the number of short-period binaries and does not effect wide binaries, the cluster dynamics does not alter short period binaries but reduces the number of wide binaries. However, after we combined the two processes, the log-uniform distribution was successfully converted to a log-normal period distribution. To prove this we performed a χ^2 -test of our evolved period distribution and the observed period distribution of Duquennoy & Mayor 1991 and obtained a probability of 89% that both distributions have been sampled from the same parent distribution.

To further generalize the results obtained for the ONC, we additionally reperformed the above mentioned simulations for clusters of varying initial stellar and gas densities. For them, we reinvestigate, if the dynamical evolution of the binary population is self-similar as described by Kaczmarek (2011) for ONC-like systems and how the shape of the period distribution differs when varying the stellar and gas-densities in the cluster.

[9] Turbulent mixing in the planetary boundary layer

J. P. Mellado, C. Ansorge, Th. Mauritsen, D. Abma, T. Heus

This poster presents three turbulence problems commonly found in the planetary boundary layer and that are relevant for the advancement of current models in climate research. All of them are studied using direct numerical simulations performed at Jülich Supercomputing

Centre.

The first one addresses unsteady convection, one aspect of the convective boundary layer. This work relates to previous research on buoyancy-driven systems in the laboratory and the atmosphere. Despite moderate Rayleigh numbers, we prove the applicability of direct numerical simulations to study this type of geophysical problems. We have defined in detail the vertical structure and we have investigated the effect of boundary conditions.

The second example considers the Ekman layer, which typifies the planetary boundary layer in the mechanically-driven limit. This work extends existing data in wall-bounded flows by increasing anisotropy and adding turbulent entrainment. When buoyancy is added, turbulence-wave interaction further complicates the system. The different regimes observed in the atmosphere are reproduced in the simulations: weak, intermediate and strong stratification. The goal is to focus on the strongly stratified limit, where turbulence collapse modifies substantially the transport between the surface and the upper, free atmosphere. This process occurs for instance in boundary layers in the Arctic.

The third example is related to shallow cumulus, one type of clouds very important in the maritime atmospheric boundary layer that develops in the tropics. In particular, we investigate the role of evaporative cooling in the lateral boundary and the so-called subsiding shell. The turbulent mixing that issues thereof creates a jet-like structure that interacts with shear-induced mixing caused by the main updraft, and the relative importance between the two of them needs to be quantified. We have obtained the time and length scales of this process and they agree with estimates from field measurements, confirming that this mechanism is relevant and models could benefit from its parametrization.

[10] Massively parallel simulations of Type Ia supernova explosions

I. Seitenzahl, F. Ciaraldi-Schoolmann, M. Fink, W. Hillebrandt, M. Kromer, R. Pakmor, F. Röpke, S. Sim

The Nobel Prize in Physics was awarded in 2011 for the discovery that the Universe is expanding at an accelerating rate. The result is based on exploiting an empirically determined relationship between the maximum luminosity and the width of the light curve of Type Ia supernovae (SNe Ia). Amazingly, the nature of the progenitor systems and the explosion mechanism remains undetermined. Therefore, a thorough study of the proposed mechanisms is required to place this cosmological application of SNe Ia on a sound theoretical basis. We contribute to this by performing massively parallel hydrodynamical simulations of SN Ia explosions and subsequent radiative transfer simulations for full star explosion models in three dimensions.

With the LEAFS code we compute three-dimensional, high resolution, full-star hydrodynamic explosion simulations for a range of different explosions models. For each simulation we derive time dependent spectra and light curves with the three dimensional Monte Carlo radiative transfer code ARTIS. Both LEAFS as well as ARTIS are multi-physics, multi-scale state of the art simulation codes with proven excellent scaling properties on JUGENE.

Using these codes we have generated for the first time a grid of three dimensional supernova simulations from ignition to emission for two of the leading explosion models for SNe Ia. The synthetic observables of such model suites allow for detailed comparison with observations and move us a big step forward in finding the progenitor systems of SNe Ia. Scrutinizing alternative explosion scenarios with the same rigorous approach is our goal for the future.

[11] Effect of the initial disc-mass distribution in star-disc encounters

M. Steinhausen, C. Olczak, S. Pfalzner

There is increasing observational evidence that most, if not all, stars are initially surrounded

by a circumstellar disc. With time the so-called protoplanetary disc becomes depleted of gas and dust and eventually disappears. Currently it is unclear which of a variety of physical mechanisms dominates this evolutionary processes. The focus of this study is on the effect of stellar encounters.

A parameter study of coplanar encounters between a disc-surrounded proto-star and a disc-less secondary star has been performed. Various disc properties like its mass or angular momentum depend on the initial disc-mass distribution. For this purpose a flexible numerical scheme has been implemented in the simulation code which allows us using one simulation for several arbitrary initial disc-mass distributions, based on a power law ansatz $\Sigma \propto r^{-p}$.

It is shown that changing the initial disc-mass distribution has a significant impact on the relative disc-mass and angular momentum losses in star-disc encounters, so that it might influence recent estimates for the evolution of star-disc systems in young stellar clusters. As a result of the parameter study a fit formula is derived, describing the relative mass and angular momentum losses dependent on the initial disc-mass distribution index p . The most significant differences between the investigated initial disc-mass distributions are found for perturbations of the outer parts of the disc by high-mass stars, while least differences are determined for disc-penetrating encounters. Maximum losses are obtained for initially flat distributed disc material. Investigating the final surface density distributions showed that encounters may produce unexpected profiles of $p \approx -1$ while also being able to cause steep profiles of $p > 2$ even in case of initially flat distributions.

The obtained results can be applied not only to the here presented examples but to *any* given disc-mass distribution. This will be particularly useful when soon upcoming observations will be able to put tighter constraints on the mass distribution in discs. Furthermore, independent of the initial disc-mass distribution encounters induce steep surface density distributions which might be the prerequisite to form planetary systems similar to our own solar system.

[12] High resolution simulations of planet formation processes: Gravoturbulent planetesimal formation on JUGENE

H. Klahr, A. Johansen, K. Dittrich, N. Raettig

We study a new scenario for the rapid formation of kilometer sized planetary building bricks, called planetesimals, based on the combined effects of magneto hydrodynamical turbulence and gravity. Meter-sized objects get concentrated by turbulence; these over-densities start to get enhanced even further due to a clumping instability and finally densities are large enough that heaps of boulders fit into their combined Roche Lobe. On JUGENE we performed the highest resolution simulations to date of dust dynamics and planetesimal formation in turbulence generated by the magnetorotational instability. We present a new domain decomposition algorithm for particle-mesh schemes. Particles are spread evenly among the processors and the local gas velocity field and assigned drag forces are exchanged between a domain-decomposed mesh and discrete blocks of particles. We obtain good load balancing on up to 4096 cores even in simulations where particles sediment to the mid-plane and concentrate in instability.

[13] Viscous versus Ohmic heating in a MHD coronal model

Ph.-A. Bourdin, S. Bingert, H. Peter

A 3D MHD coronal model driven by photospheric observations is set up to synthesize coronal emission for later comparison with real observations of the coronal structure and dynamics. We start with a hydrostatic stratified atmosphere, a Hinode/SOT magnetogram of a full active region as a lower boundary condition, and drive the magnetic field by photospheric granular motions. The braiding of fieldlines induces currents and leads to Ohmic dissipation that drives

the dynamics of the corona and determines its thermal structure. Inclusion of gravity, field-aligned heat conduction, and radiative losses in the energy balance allows to determine the pressure in coronal structures. Coronal emission is synthesized using the CHIANTI atomic database. The comparison between the synthesized X-ray and EUV emission with the observed emission patterns and their Doppler shifts in the lines e.g. Fe VIII, Fe XII, Fe XV, and Ca XVII will provide a crucial test for the assumed heating mechanism, especially the energy input distributed in space and time, e.g. Ohmic heating in nanoflares. Early results are used to investigate the distribution in space of viscous and Ohmic heating.

[14] The influence of partial melting on the thermo-chemical evolution of terrestrial bodies of terrestrial bodies

N. Tosi, A.-C. Plesa, M. Laneuville

Solid-state mantle convection is the primary mechanism that controls the dynamics and thermal evolution of the Earth and terrestrial planets. Thermal and compositional buoyancy drive the slow creeping flow of the silicate mantle of planetary bodies and are responsible for the heat transport efficiency, magnetic field generation and formation of geological structures such as volcanoes, rifts and tectonic plates.

Mantle convection takes different forms on different planets. Besides Earth, where the lithosphere (the outer rigid layer of the planet) is broken in seven major plates that participate in the mantle convection cycle, on all other terrestrial bodies of the Solar System, convection does not involve the outermost layers. It occurs instead below an immobile lid - the stagnant lid - across which heat is transported by conduction and that acts as an insulating layer which keeps the mantle warm.

In a developed convective regime, the temperature of regions of the upper mantle, either below tectonic plates or a stagnant lid, often lies near or slightly above the solidus - the temperature at which the mineral with the lowest melting temperature among those that form the silicate mantle mixture starts to melt. Over the range between the solidus and the liquidus - the temperature above which all mixture constituents melt - both a solid and a liquid phase coexist to form a partially molten aggregate. The different styles of mantle convection affect strongly the generation of partial melt. This, in turn, influences the cooling behaviour and convective structure itself, creating important feedback mechanisms that can impact the overall thermal evolution of a planet. Partial melting affects not only the melting temperature itself causing the solidus to increase as the degree of melting increases, but also causes dehydration of the mantle by partitioning of water from the minerals into the melt, it is accompanied by compositional variations due to mantle depletion in incompatible elements and by fractionation of radiogenic heat sources between mantle and crust.

We concentrate our efforts on modeling the thermo-chemical evolution of Mercury, the Moon and Mars, accounting for partial melting and using constraints derived by the analysis of recent data from space missions such as MESSENGER, Lunar Reconnaissance Orbiter or Mars Express. To this end, we use the 2D cylindrical - 3D spherical convection code Gaia [1, 2, 3]. To simulate the effects of partial melting, we use a particle-in-cell approach [4] by tracking the motion of particles whose distribution defines the solidus, compositional variations, water concentration and radioactive heat-sources.

[1] Hüttig C., & Stemmer K. (2008). G3, 9(2), Q02018.

[2] Hüttig C., & Stemmer K. (2008). PEPI, 171(1-4), 137-146.

[3] Plesa, A.-C. (2011). INFOCOMP Proceedings, 167-172.

[4] Plesa, A.-C., Tosi, N. & Hüttig, C. (2012). In Review.

[15] The plasma environment of the comet 67P/Churyumov-Gerasimenko

Ch. Koenders, K.-H. Glaßmeier

In 2014, the European spacecraft ROSETTA will arrive at the comet 67P/Churyumov-Gerasimenko, where it will deliver the PHILAE lander and start to escort the comet to its perihelion. Among many other instruments, there are two magnetometer experiments on board, which were built and are being supervised by the Institute for Geophysics and extraterrestrial Physics at the University of Braunschweig (Glassmeier et al., 2007; Auster et al., 2007). These instruments allow us to gain a deeper insight into the evolution of the complex interaction between a comet and the solar wind.

The interaction arises because the comet builds an extended exosphere when it approaches the sun. Solar UV-radiation leads to the ionisation of the neutral molecules in this exosphere. The interaction between the newly born cometary ions and the impinging solar wind leads to the formation of different structures and boundaries, e.g. the bow shock, the magnetic pile up boundary, the diamagnetic cavity and the plasma tail beyond the nucleus. With the instruments on ROSETTA we will be able to study these structures and boundaries. Moreover, we will observe the evolution of the comet, from an inactive to an active comet.

Since the interaction of weak comets is dominated by kinetic effects, we use the A.I.K.E.F. simulation program, which is based on the hybrid approach. This model describes the ions as particles and the electrons as a massless fluid. However, expensive numerical simulations are necessary to simulate the interaction in order to obtain reasonable estimations of the position and properties of the boundaries and the structures in the cometary environment. This knowledge will be used for the mission planning of the ROSETTA spacecraft to prepare the required trajectories for the measurements and to ensure the scientific success of this unique mission.

Auster, H. U., Apathy, I., Berghofer, G., Remizov, A., Roll, R., Fornacon, K. H., Glassmeier, K. H., Haerendel, G., Hejra, I., Kühr, E., Magnes, W., Moehlmann, D., Motschmann, U., Richter, I., Rosenbauer, H., Russell, C. T., Rustenbach, J., Sauer, K., Schwingenschuh, K., Szemerey, I., Waesch, R., 2007, ROMAP: Rosetta Magnetometer and Plasma Monitor, *Space Science Reviews*, 128, 221–240.

Glassmeier, K., Richter, I., Diedrich, A., Musmann, G., Auster, U., Motschmann, U., Balogh, A., Carr, C., Cupido, E., Coates, A., Rother, M., Schwingenschuh, K., Szegö, K., Tsurutani, B., 2007, RPC-MAG The Fluxgate Magnetometer in the ROSETTA Plasma Consortium, *Space Science Reviews*, 128, 649–670.

[16] Plasma and dust simulations on the saturnian rings

P. Meier, H. Kriegel, St. Wiehle, Y. Vernisse, U. Motschmann

A wide range of methods is available to numerically model space plasma processes. Dealing with scales comparable to ion gyration radii (e.g. comets, Titan or Enceladus), a hybrid model is the most convenient choice. It treats the electrons as a fluid, whereas a completely kinetic approach is retained to cover ion dynamics. From the numerical point of view, it can be categorized as a particle-mesh code. The particles which represent the ions interact with the electromagnetic fields defined on the numerical mesh.

Enceladus is a moon within Saturn's E-ring embedded in a plasma environment. Measurements of the Cassini spacecraft have shown that water vapor and ice particles are ejected from the south polar regions through geysers. Thereby a dust plume is generated which supplies the E-ring with dust. Cassini's Cosmic Dust Analyzer (CDA) can detect this dust until a lower threshold of micrometers of dust radii. Measurements with Cassini's plasma instrument (RPWS) show higher ion than electron densities of the plasma environment, since

the dust is mainly negatively charged. However, the detected dust carries too little charge for explaining this difference implying the necessity of submicrometer dust. So simulations for the submicrometer dust and charging processes are necessary. We present such hybrid simulations of the plasma interaction with Enceladus' plume. Our results are compared with Cassini Magnetometer (MAG) data in order to understand the size distribution of the dust.

Plasma Physics

[17] Controlled electron-beam injection into plasma waves for tailored betatron-radiation generation

T. Mehrling, J. Grebenyuk, J. Vieira, J. L. Martins, R. A. Fonseca, L. O. Silva, J. Osterhoff

Plasma acceleration of electron beams is a quickly emerging field with potential applications such as driving tabletop X-ray light sources or even compact future particle colliders. Laser wakefield acceleration (LWFA) is a plasma acceleration method that exploits high intensity laser fields for the ionization of gas targets and the excitation of large amplitude plasma waves.

Even though its prospects are promising, plasma acceleration is currently still in a state of infancy. At present, producing electron beams of applicable quality remains a significant challenge. This can be attributed to a lack of control over the particle injection mechanism. A solution might be the external injection of conventionally pre-accelerated electron bunches into plasma waves, as planned at DESY, which offers a new degree of control over the injection process and might thus lead to improved beam quality. This technique also provides unique possibilities for light generation from plasma wakes, longitudinal bunch compression, or comparative investigations between the state of the electron bunch before and after the acceleration process, as is needed e.g. for studies of emittance growth. Moreover, external injection is key to the mastering of staging of LWFA modules.

The interaction of high intensity laser beams with plasma is a highly nonlinear kinetic process that can only be understood in detail by the use of simulations. Numerical emulation of the dynamics of large numbers of particles in their self-consistent fields place high demands on computational resources as well as on the parallelization of the code. OSIRIS is a three dimensional, relativistic and massively parallel particle-in-cell (PIC) code, developed at Instituto Superior Técnico in Lisbon, Portugal, designed to simulate such processes.

We present preliminary results of PIC simulations performed with the code OSIRIS on JUGENE as well as simulations planned at JUGENE that explore and analyze in detail external bunch injection and the resulting possibilities mentioned before.

[18] Thomson scattering on inhomogeneous targets

P. Sperling, D. Bauer, T. Döppner, C. Fortmann, S.H. Glenzer, T. Liseykina, A. Pukhov, R. Thiele, S. Toleikis, Th. Tschentscher, and R. Redmer

The introduction of free electron lasers enables new pump-probe experiments to characterize warm dense matter, i.e. systems at solid-like densities and temperatures of several eV. For instance, such extreme conditions are relevant for the interior of giant planets and along the compression path of inertial confinement fusion capsules. Due to strong correlations and quantum effects a theoretical treatment of warm dense matter is rather complicated so that consistent methods of many-body physics have to be applied. Theoretical results for the pair distribution functions and the equation of state can now be checked using new experimental techniques. For instance, within ongoing experimental campaigns, a short-pulse optical laser irradiates a target, e.g. liquid jets (at FLASH) or thin foils (at LCLS), that is subsequently probed with brilliant X-ray radiation. The inhomogeneous plasma prepared by the optical laser is characterized with particle-in-cell simulations. The interaction of the X-ray probe radiation with the inhomogeneous plasma is also taken into account for different time delays between pump and probe via radiative hydrodynamic simulations.

For the pump-probe experiments performed at FLASH on liquid hydrogen (helium), we calculate the respective scattering spectrum based on the Born-Mermin approximation for the dynamic structure factor considering the full density and temperature dependent Thomson

scattering cross section throughout the target. We can identify plasmon modes that are generated in different target regions and monitor their temporal evolution. Combining these results with the ion signal the temperature equilibration between electrons and ions can be studied as well. Therefore, such pump-probe experiments are promising tools to measure not only the important plasma parameters density and temperature but also to gain valuable information about their time-dependent profile through the target. The method described here can be applied to various pump-probe scenarios by combining optical lasers, soft and hard X-ray sources.

Hydrodynamics and Turbulence

[19] Combining fluid dynamics with the tree-code PEPC

A. Breslau, M. Winkel, L. Arnold, P. Gibbon, S. Pfalzner

Stars form by gravitational collapse of giant interstellar gas clouds. Due to angular momentum conservation discs consisting of gas and dust form during this process around the young stars. Due to the potential of later formation of planets out of the disc-material they are called protoplanetary discs. Several processes are known to influence the further evolution of these discs, e.g. photoevaporation, star-disc encounters or chemical evolution of the disc material.

To investigate the exact interplay of these processes, simulations of protoplanetary discs are performed. Therefore simulation codes are needed, which combine at least a gravity and a fluid dynamics solver. To run simulations with very high resolution on JSC's highly parallel supercomputers, the parallel tree-code PEPC, which can be used as a gravity solver, was combined with a particle based fluid solver (SPH).

To demonstrate, that the code produces correct physical results, several common test problems were investigated. It was shown, that the code can propagate sound waves with only small deviations from the analytical solution and that the code can resolve shock waves sufficiently. Further, the correct cooperation of the new and old code components were demonstrated.

[20] Optimal noise-control of plane jets using adjoint-methods

H. Foysi

A control optimization technique using the continuous adjoint of the compressible Navier-Stokes equations was implemented for aeroacoustic optimization of plane jet flows. The purpose of the adjoint equations is to provide sensitivity information, which is afterwards used in a gradient-based minimization of a prescribed cost functional, designed to describe the far-field sound pressure level (SPL).

The continuous adjoint calculation makes use of the commonly used first-optimize-then-discretize approach, which is known to involve inaccuracies due to inconsistencies in the discretized systems. The objective of the present work was to demonstrate the ability to reduce the sound in the near far-field of plane jets on the one hand, and to investigate the accuracy of the continuous adjoint approach on the other hand. The considered cases exhibit a nozzle exit Reynolds number of $Re=2000$ and a Mach number of $M=0.9$, performed using two-dimensional direct numerical simulation and three-dimensional large-eddy simulation, respectively.

A comparison of the obtained gradient via adjoint and finite differences is presented and it is shown, that in order to obtain reliable gradient directions, the length of the optimization time needs to be restricted. Furthermore, a receding horizon optimization for the two-dimensional plane jet simulation is used to obtain a sound reduction over much longer time intervals.

[21] Efficient solvers for massively parallel simulation of continuum models for flow and transport

V. Aizinger, I. Heppner, M. Lampe, A. Nägel, S. Reiter, M. Rupp, A. Vogel, G. Wittum

One key challenge in many application-oriented simulations is the solution of large linear systems of equations. This task is typical for models based on partial differential equations or integral equations as they occur in numerous models in science. The efficiency of this solution

process is often a decisive and critical step for the overall complexity of the simulation process.

Although nowadays (super-) computing resources provide an enormous potential, an in-depth exploration of this potential is only possible by efficient, mathematically well-founded methods and algorithms. For large problems, e.g., a direct application of standard methods often leads to deficient results, as, e.g., computational complexity does not scale linearly with the problem size or the structure of the problem is not reflected appropriately.

We present geometric and algebraic multigrid approaches, which are designed for robustness and scalability. First numerical results for model problems indicate, that these approaches can be run efficiently on JUGENE on up to 64Ki cores.

[22] Scale-by-scale energy budget equations for the mixing of a passive scalar by homogeneous turbulence

M. Gauding, A. Wick, J. H. Göbbert and N. Peters

The mixing of a passive scalar with imposed mean gradient by steady homogeneous turbulence is investigated by means of a scale-by-scale scalar energy budget equation in the context of large-eddy simulation (LES). The turbulent energy transport between scales is a crucial quantity which has to be satisfied by sub-grid closures in order to preserve the statistical properties of the flow field. The scalar scale-by-scale energy budget can be expressed by the transport equation of second moment of the scalar increment written in a generalized form accounting for the mean gradient. For comparison with LES a new scale-by-scale scalar energy budget equation for the filtered second order moment of the scalar increment is derived. This equation incorporates the balance between production at large scales due to the mean gradient, transport at intermediate scales, as well as diffusion at small scales. For LES, diffusion divides into a viscous and a sub-grid part. Based on this equation an a posteriori comparison of LES with filtered direct numerical simulation (DNS) is conducted. An eddy-viscosity sub-grid closure reveals very good agreement for all scales. For reference also the results from DNS are discussed. The effect of the molecular diffusivity is studied by varying the Schmidt number between 0.25 and 6.

[23] Alignment of dissipation elements in a turbulent channel flow

J. H. Göbbert, M. Gauding, N. Peters

There have been many attempts to define the structure of geometrical objects in turbulence. For three-dimensional flows geometry can be represented as point, line, surface or volume. Examples of geometrical structures are stagnation points, streamlines, iso-surfaces or vortex tubes. A volumetric object called dissipation element was introduced by Wang and Peters (2006) [1], which is defined by all that points from which gradient trajectories reach the same minimum and maximum point of a scalar field. The statistics of dissipation elements of the kinetic energy field in different turbulent flows have been analyzed extensively lately [2].

In this work the alignment of dissipation elements with respect to local strain rate, the distance to the wall and other geometrical structures was examined. Therefore a code for direct numerical simulations of a turbulent channel flow was developed based on the algorithm of Kim Moin Moser (1987) [3] for highly resolved DNS of $\delta x/\eta = 1.0$ and $Re_{\tau} = 590$ to run on JUGENE at the Forschungszentrum Jülich with up to 16384 CPUs.

[1] L. Wang, N. Peters. The length scale distribution function of the distance between extremal points in passive scalar turbulence, *J.Fluid Mech.*, 554:457-475, 2006.

[2] M. Gampert, J. H. Göbbert, P. Schaefer, M. Gauding, N. Peters, F. Aldudak, M. Oberlack. Extensive strain along gradient trajectories in the turbulent kinetic energy field. *New Journal of*

Physics, 13, 043012, 2011.

[3] J. Kim, P. Moin, R. Moser. Turbulence statistics in fully developed channel flow at low Reynolds numbers. *J. Fluid Mech.*, 177, 133-166, 1987.

[24] Impact of bypass-duct bifurcations on fan noise

A. Holewa, Ch. Weckmüller, Sébastien Guérin, L. Enghardt

A typical aircraft-engine bypass contains components such as struts and bifurcations. The present work is focused on the impact of the potential field of the bypass bifurcations on rotor tonal noise. Two configurations are compared at take-off condition by means of quasi-3D steady and unsteady RANS calculations: The first configuration represents an isolated rotor-stator stage; the second configuration appends the same rotor-stator stage by a section of the bypass duct containing struts, a lower and an upper bifurcation. It is shown that the bypass duct components impose backwards circumferentially non-uniform flow conditions on the rotor, which lead to a significant change of the modal structure of the acoustic field at the blade passing frequency and its harmonics in the bypass duct. Furthermore the shock position on the rotor blades is changed during the rotation which could influence the source mechanism of buzz-saw noise.

[25] Highly efficient and scalable software for the simulation of turbulent flows in complex geometries

D. F. Harlacher, S. Roller

The BMBF funded project STEDG is concerned with turbulent flows originating from complex geometries. The targeted goal of the presented project is the aero-acoustic design of a natural gas injector. Here, we have to consider super-sonic flows with shocks (discontinuities), as well as large discrepancies in scales between flow and acoustics. This requires a high resolution and/or approximation order in space and time. Within the project, we use Large Eddy Simulation (LES) to model the turbulent effects and a high order Discontinuous Galerkin discretization due to its low dispersion which is necessary to treat the wave propagation correctly. The solver code HALO, developed by IAG, Uni Stuttgart and GRS, is based on unstructured grids to represent the complex nozzle geometry.

Due to its high resolution requirements, the simulation is computationally demanding. We therefore investigate the influence of mesh refinement (h-adaptivity) vs. increasing the order of accuracy (p-refinement) on the quality and efficiency of the simulation. Efficiency here is thought in numerical meaning, i.e. quality vs. stability, as well as in parallel scalability and single-CPU efficiency. The code requires direct neighbour communication only. Time integration is based on a local time stepping scheme, therefore also avoiding global (all-to-all) communications. The code has shown highly suitable for current and future multi- and many-core machines with large numbers of cores. It scales up to 4096 cores on JUROPA, with a typical mean job size using 1024 cores. Results are shown for different discretizations and orders.

[26] Turbulent convection with phase changes including precipitation and radiative transfer

Th. Weidauer, O. Pauluis, J. Schumacher

Conditionally unstable convection occurs when the stratification is stable for unsaturated air parcels but unstable for saturated air parcels. This leads to the development of isolated

convective plumes or clouds which are separated by an extended unsaturated dry environment. Here the statistical behaviour of conditionally unstable convection is studied in a model of moist turbulent convection with a simplified thermodynamics of cloudy air. It is closely related to the classical Rayleigh-Benard convection problem, but includes phase transitions between the gaseous and liquid phase and the effect of latent heat release on the buoyancy of air parcels. We investigate the impacts of radiative cooling and precipitation on the self-sustained convective regimes. Therefore a simple steady bulk cooling scheme is added to the advection-diffusion equations for the scalar fields or liquid water is removed when a certain threshold is exceeded.

[27] Modeling and simulation of turbulent primary atomization for evaporating spray

P. Zeng, H. Pitsch, B. Binninger, N. Peters, M. Herrmann

Low-NO_x and smokeless combustion is one of the most important objectives of designing new generation bio-fuels, and an advanced mixture formation strategy is the key to reduce the combustion emissions. Since fuel injection is the best way to control mixing, the fundamental physics of the injection process, such as liquid primary atomization should be studied. In this research project, we numerically investigate the influence of fuel properties on spray formation, injection induced turbulence, as well as heat and mass transfer. The computational fluid dynamics (CFD) models are carefully chosen to fulfill the accuracy requirements of simulating the multi-scale flow field. Our approach uses the ensemble thermal properties of fuel molecules (e.g. density, viscosity, surface tension, specific heat, etc.) plus transport properties (e.g. diffusivity, conductivity, etc.) as inputs, and provides the mixture field information, namely the spray structures, turbulence, mixture fraction and temperature as outputs. We find that the surface tension plays the major role in defining the primary atomization characteristics.

Acknowledgement:

This work was performed as part of the Cluster of Excellence "Tailor-Made Fuels from Biomass"-TMFB, which is funded by the Excellence Initiative of the German federal and state governments to promote science and research at German universities.

[28] Finite size particles in homogeneous turbulence

T. Doychev, M. Uhlmann

In the present work we have investigated finite size and finite Reynolds number effects of particle laden turbulent homogeneous flow by direct numerical simulation. The terminal particle Reynolds number Re_D based upon the particle diameter, the particle terminal velocity w^∞ and the fluid kinematic viscosity ν is of order of $O(100)$. The particle terminal velocity w^∞ is defined as the settling velocity of a single particle in an ambient fluid based on the balance between drag and buoyancy using the standard drag formula from [1]. Under these conditions, the point-particle approach loses its validity and in order to describe the flow the interface between the dispersed- and carrier-phase is fully resolved by means of the immersed boundary method [2]. In this work the two-phase flow is dilute, i.e. the volume fraction is set to be below 0.5 %. Therefore dominant effects of inter-particle collisions are avoided.

In order to better understand the effect of turbulence generation through the particles, first the settling of heavy finite size particles in an ambient fluid was simulated. Thus the contribution of the particle wakes to the flow field turbulence is investigated. In this study the analysis will focus on three topics: (i) what is the statistical description of the particle wakes, (ii) what is the spatial structure of the dispersed phase (cluster formation, preferential concentration) and (iii)

what is the effect of the presence of multiple particles on the particle settling velocity. In this work particular care has been taken to meet the resolution requirements (small scales, box size and time step) of the two-phase flow.

[1] Clift R., Grace J. R. and Weber M. E., (1978), Bubbles, drops and particles, Academic Press.

[2] Uhlmann M., (2005): An immersed boundary method with direct forcing for the simulation of particulate flows, J. of Comp. Phys., vol 209, pp. 448-476.

[29] Hydrodynamics of falling liquid films with periodic 3-dimensional surface waves

G. F. Dietze, W. Rohlf, R. Kneer

Falling liquid films (i.e. thin layers of liquid accelerated by gravity and flowing along a bounding wall) play an important role for a number of technical applications such as wetted-wall cooling towers, falling film evaporators and packed-bed columns. Such flows are characterized by a convective long-wave instability resulting from inertia as well as from the non-symmetrical effect of gravity. This instability leads to the development of interfacial waves, which according to Squire's theorem are two-dimensional at the onset yet develop into three-dimensional structures further downstream. These structures exhibit large horseshoe-shaped wave fronts preceded by a number of capillary waves (so named due to the relevance of capillary forces). Although this general phenomenology has been established for some time, the physical mechanisms leading to the development of three-dimensional interfacial deformations remain yet to be identified. Further, their effect on the velocity field within the liquid phase needs to be elucidated in order to support modeling assumptions in the context of integral boundary layer models and clarify the wave-induced convective scalar transport (and associated transfer) intensification in three-dimensional falling liquid films.

It is with this in mind that a number of fully resolved numerical simulations of the Navier-Stokes equations (in both the liquid and gaseous phase) within periodic wave segments of three-dimensional laminar falling liquid films were planned for the current grant period. The considered flow conditions are based on cases previously investigated experimentally by Park and Nosoko (AIChE Journal, vol. 49, no. 11, 2003, p. 2715). To account for the two-phase character of the flow, the Volume of Fluid (VOF) and Continuum Surface Force (CSF) methods were employed within the finite volume based solver OpenFOAM 1.7. One of these simulations has been completed and is the subject of this contribution. Results display good agreement with the experimental visualizations of Park and Nosoko (2003). Further, the obtained data exhibit a complex and segregated three-dimensional wave topology with regions dominated by capillary forces separated from regions dominated by inertia. Meanwhile, the associated velocity field displays a complex structure of vortices that could represent a transition path toward turbulence in falling liquid films and might be responsible for the substantial intensification of heat and mass transfer in the considered flows.

Environmental Research

[30] Convection-permitting climate simulations for North Africa

I. Bischoff-Gauß, N. Kalthoff, V. Klüpfel, H.-J. Panitz, L. Gantner

A great challenge for forecast and climate models is the simulation of the amount and distribution of precipitation. Regarding the different types of precipitation the simulation of convective precipitation is the most difficult one. In West Africa, mesoscale convective systems (MCSs) are an important component of the West African monsoon system, because convective precipitation contributes predominantly to the annual rainfall. Therefore, for West Africa a discrepancy between the simulation skill of precipitation and the economic, society-environmental needs for a precise forecast of the onset of the summer monsoon as well as of the reproduction of the African climate exists.

During the last years some progress in modelling convection has been made by convection-permitting models, which were applied to process studies and restricted areas. However, there is still a lack of convection-permitting simulations for the climatological scale. A step to fill this gap can be done within the framework of CORDEX (Coordinated Regional climate Downscaling Experiment), for which Africa is a key region of interest. However, during the first phase of CORDEX simulations with the much coarser resolution of 50 km are executed. One of these models is COSMO (Consortium for small scale modelling), applied in the climate mode COSMO-CLM (CCLM). Although all models more or less capture the bi-modal structure of the annual precipitation cycle, their results vary within a broad band around the satellite derived observations. The reasons for the discrepancies are unclear. Therefore the subjects of this project are to investigate whether (i) convection-permitting simulations significantly improve the representation of the observed daily and annual cycle of precipitation over North Africa and (ii) an impact of model initialisation and boundary conditions on the simulation of precipitation exists.

During the first phase of the project, model simulations with CCLM were performed with a horizontal resolution of 2.8 km for North Africa for 2006. First comparisons of the simulation results with satellite-derived data of the annual precipitation sum show that the simulations quite well represent the observed spatial distribution, especially, e.g. the orographically initiated convective precipitation over the plateau of Ethiopia and along the border of Nigeria and Cameroon. Also, the comparisons of simulated annual cycle of temperatures and specific humidity with measurements for characteristic climate regions, like the Guinea coast, the Soudanian and the Sahelian zone show promising similarities. In the next step detailed analyses will be performed to investigate the main differences, including the daily cycle of temperature, humidity and precipitation between the simulation with convection parameterisation (50 km resolution) and convection-permitting simulations (2.8 km).

[31] The role of zonation of river bed conductivities on river-aquifer exchange fluxes and on state-parameter updates with the Ensemble Kalman Filter

W. Kurtz, H.J. Hendricks Franssen, H. Vereecken

A proper characterization of river-aquifer exchange fluxes is important for groundwater management because of their influence on regional water balance and groundwater quality. Different studies have shown that the heterogeneous distribution of hydraulic conductivities around or within a river bed strongly influences the exchange fluxes between river and aquifer. However, it is often unclear how much heterogeneity has to be represented in a model in order to achieve an adequate representation of river-aquifer interactions. We performed a sensitivity analysis for the effect of zonation of river bed conductivities (L) on the

characterization of aquifer states in a Monte Carlo framework. Additionally, data assimilation techniques were used to improve model predictions and model parameters for the different zonation approaches. For our synthetic simulation experiments we used a 3D finite element model of the Limmat aquifer in Zurich (Switzerland) which includes river-aquifer exchange as well as groundwater management activities such as bank filtration and artificial recharge. Ten synthetic L -fields were generated which showed a rather high degree of spatial variability (standard deviation: $\sim 1.7 \log_{10}(\text{m s}^{-1})$). Reference runs with these synthetic L fields (total simulation period: 609 days) yielded the basis for the comparison of the different zonation approaches. Different ensembles were generated that either reproduced the full heterogeneity of the reference fields (457 leakage zones) or where the number of leakage zones was reduced to 5, 3 or 2 zones. These ensembles were propagated forward in time either without updating (open-loop simulations) or using 100 head data for updating hydraulic heads and leakage coefficients of the different ensembles with the Ensemble Kalman Filter (EnKF). Results from unconditional simulations showed that all four zonation approaches led to approximately comparable errors with respect to reference runs. When EnKF was used to jointly update hydraulic heads and L values the decrease in hydraulic head errors was more pronounced for the more spatially distributed zonations (i.e., 457 and 5 zones) than for 3 and 2 zones where the errors showed a more systematic character. This is most likely related to the fact that for the 457/5 zones the general spatial patterns of the reference fields are still resolved by the ensemble whereas for 3/2 a stronger spatial averaging takes place. The net fluxes between river and aquifer were also adequately represented by the 457 and 5 zone ensembles whereas for 3 and 2 zones the net fluxes were underestimated for most of the reference runs. The updating behaviour of L during the simulation period showed that the ensemble with 457 zones converged towards the spatial structure of the reference fields. In contrast, the ensemble variance for 5, 3 and 2 zones decreased rather fast. In summary, it is concluded that a higher spatial distribution of leakage zones generally leads to a better performance of EnKF in river-aquifer systems in terms of state and parameter prediction. Nevertheless, EnKF is able to correct in part for an incorrect parameterization of riverbed heterogeneity, but this mainly concerns the hydraulic head values, whereas the parameter values are only significantly improved when basic spatial features of the true L -field are represented correctly.

[32] Next generation regional climate scenarios for the greater alpine region (ReCliS:NG) – concept and first results

M. Suklitsch, H. Truhetz, A. Gobiet

In 2007 the European Union (EU) settled on a "2° C target": mitigation scenarios of anthropogenic greenhouse gas emissions should be employed limiting the global warming to 2° C. Until now emission scenarios did not include any mitigation initiatives. In the recent years the "representative concentration pathway" (RCP) scenarios [1] were designed to include mitigation strategies and are currently used as driving data in global climate projections for the upcoming 5th Assessment Report of the IPCC.

In the project "Next Generation Regional Climate Scenarios for the Greater Alpine Region" (ReCliS:NG) [2], funded by the Austrian Climate Research Programme (ACRP), the meteorological model COSMO-CLM [3] is used as regional climate model (RCM) to derive highly resolved (10 km × 10 km grid spacing) climate change information in the Alpine region based on the novel RCP scenarios. A total of 3 simulations is currently conducted at the Jülich Supercomputing Centre (JSC): One hindcast for the period 1989 to 2010 using the re-analysis dataset ERA-Interim [4] as driving data and two climate simulations for the period 1955 to 2100 using different RCP scenarios: one which meets the "2° C target" and one which includes less ambitious mitigation initiatives. Since RCMs are known to feature considerable errors, empirical-statistical correction methods will be applied as well. The simulations will be evaluated and a climate change analysis will be conducted comparing the two different

scenarios and linking them to the existing pool of Austrian climate change scenarios. The poster lays out the concepts of the on-going project ReCliS:NG and provides first results.

[1] M. Meinshausen, S. J. Smith, K. V. Calvin, et al., The RCP Greenhouse Gas Concentrations and their Extension from 1765 to 2300, *Climatic Change* 109, 213–241, 2011, doi: 10.1007/s10584-011-0156-z.

[2] M. Suklitsch, A. Gobiet, M. Themel, H. Truhetz, ReCliS:NG Next Generation Regional Climate Scenarios for the Greater Alpine Region, International Conference on the Coordinated Regional Downscaling Experiment (CORDEX), Mar 20 Mar 26, 2011, Trieste, Italy.

[3] U. Böhm, M. Kücken, W. Ahrens, et al., CLM - The Climate Version of LM: Brief Description and Long-Term Applications, *COSMO Newsletter* 6, 225–235, 2006.

[4] A. Simmons, S. Uppala, D. Dee, S. Kobayashi, ERA-Interim: New ECMWF reanalysis products from 1989 onwards, *ECMWF Newsletter* 110, 25–35, 2007.

Chemistry

[33] TRAVIS - A free analyzer and visualizer for Monte Carlo and molecular dynamics trajectories

M. Brehm, B. Kirchner

We present TRAVIS ("TRajjectory Analyzer and VISualizer"), a free program package for analyzing and visualizing Monte Carlo and molecular dynamics trajectories. The aim of TRAVIS is to collect as many analyses as possible in one program, creating a powerful tool and making it unnecessary to use many different programs for evaluating simulations. This should greatly rationalize and simplify the workflow of analyzing trajectories. TRAVIS is written in C++, open-source freeware and licensed under the terms of the GNU General Public License (GPL v3). It is easy to install (platform independent, no external libraries) and easy to use. TRAVIS has been published recently [1] and can be obtained from <http://www.uni-leipzig.de/~travis>. On this poster, we introduce some of the algorithms that are implemented in TRAVIS - many of them widely known for a long time, but some of them also to appear in literature for the first time.

[1] M. Brehm and B. Kirchner: "TRAVIS – A free Analyzer and Visualizer for Monte Carlo and Molecular Dynamics Trajectories". *J. Chem. Inf. Model.* **2011**, 51 (8), pp 2007–2023.

[34] Internal dynamics in endohedral metallofullerenes as studied by *ab initio* Born-Oppenheimer Molecular Dynamics

A. A. Popov

DFT-based Born-Oppenheimer molecular dynamics is applied to study the internal dynamics of a series of endohedral clusterfullerenes at room temperature. The list of studied molecules included endohedral metallofullerenes, including carbide clusterfullerenes $\text{Sc}_2\text{C}_2@C_{82}$, $\text{Sc}_3\text{C}_2@C_{80}$, $\text{Sc}_4\text{C}_2@C_{80}$, nitride clusterfullerenes $\text{Sc}_3\text{N}@C_{80}$, $\text{ScY}_2\text{N}@C_{80}$, $\text{TiY}_2\text{N}@C_{80}$, and one oxide clusterfullerene, $\text{Sc}_4\text{O}_2@C_{80}$. The use of the computational facilities of the Jülich Supercomputing Centre along with the fast and efficient computational procedures implemented in CP2K code enabled us to extend the propagation time up to 50 ps while pertaining reliable level of theory (namely, PBE/DZ2P). At this time scale, dynamics of the endohedral clusters inside carbon cages can be followed with great details and the influence of the cluster composition and the cage size can be revealed. In particular, we have found completely different rotational behaviour of the cluster in a family of carbide clusterfullerenes, which ranges from the rotation around the one axis in $\text{Sc}_2\text{C}_2@C_{82}$ to free 3D rotation in $\text{Sc}_3\text{C}_2@C_{80}$ to the hindered librational motions in $\text{Sc}_4\text{C}_2@C_{80}$. In nitride clusterfullerenes, substitution of two Sc atoms by two larger yttrium atoms did not change the free rotation of the M_3N cluster, but when the Sc atom in ScY_2N cluster was substituted by Ti, rotation of the cluster was changed from 3D to the librational motions around the Ti–N bond. Finally, in the oxide clusterfullerene $\text{Sc}_4\text{O}_2@C_{80}$ rotation of the cluster is hindered in the same way as it is found in $\text{Sc}_4\text{C}_2@C_{80}$, which indicates that tetrahedral metal clusters tend to exhibit similar dynamics properties despite the different electronic and geometrical properties of the non-metal atoms. Our results thus partially fill the gap between the results of static DFT computations and experimental ESR and NMR studies which give information on the internal dynamics on the nanosecond timescale. Our results can be also used to fit and validate cheaper semiempirical approaches which can then be employed for molecular dynamics studies with much longer propagation time.

[35] Structural insights into binding and resistance development of oxazolidinone antibiotics

J. Saini, S. Fulle, H. Gohlke

The ribosome is an attractive target for several antibiotics which inhibit protein synthesis by binding to the peptidyl transferase center (PTC) and exit tunnel of the large ribosomal subunit. In the last two decades, several high resolution crystal structures of antibiotics bound to ribosomal structures of different bacterial, archaeal and eukaryotic species became available. These complexes provide insight regarding binding sites, binding modes, and mechanisms of action of these antibiotics. Although, the nucleotides forming the PTC are highly conserved between these species, relatively subtle changes of rRNA arrangements yield significant resistance development [1]. Structural determination by X-ray crystallography only provides *static* views of the binding processes but does not reveal the *dynamics* involved in antibiotics binding, or energetic determinants of binding. Theoretical and computational approaches such as molecular dynamics (MD) simulations in combination with free energy calculations are suitable to fill this gap [2].

In the present study, we aim at investigating the determinants of binding and resistance of antibiotics belonging to the oxazolidinone class, the one of the only three new classes of synthetic antibiotics that have entered the market during the past 40 years [3]. In particular; we investigate linezolid, its derivative radezolid, and the structurally related oral anticoagulant drug rivaroxaban in complex with the *H. marismortui* [4] 50S subunit by means of MD simulations. Furthermore, we are investigating the influence of mutations that do not directly interact with linezolid but are responsible for its *resistance*; particularly the nucleotides corresponding to two of these mutations G2032C and C2499U (*H. marismortui* numbering) are already present in the 28S rRNA of *Homo sapiens*.

Our results show that radezolid forms more stable hydrogen bonds with a binding site residue (nucleobase G2540) than linezolid, which may be the reason for its 100-fold stronger binding affinity. In contrast, no hydrogen bond at all is observed in the case of rivaroxaban. Both linezolid and radezolid stabilize the conformation of nucleobase U2620 by forming weak hydrogen bonds, thereby preventing the correct positioning of the PtRNA and inhibiting protein synthesis. In the case of rivaroxaban, the nucleobase U2620 undergoes large movements and forms no stable interaction. Furthermore, both linezolid and radezolid show critical aromatic stacking interactions required for binding, which are missing for rivaroxaban. The analysis of hydrogen bonds and aromatic stacking interactions also provides an explanation as to why the core of linezolid and radezolid is found to be largely immobile (RMSF < 1.5 Å), while the core of rivaroxaban shows large fluctuations (RMSF ~ 3.0 Å).

[1] K. P. McCusker, D. G. Fujimori, ACS Chem. Biol. (2012), 7, 64-72.

[2] H. Gohlke, D. A. Case, J. Comput. Chem. (2004) 25, 238-250.

[3] R. C. Moellering, Ann. Intern. Med. (2003) 138, 135-142.

[4] J. A. Ippolito *et. al*, J. Med. Chem. (2008) 51, 3353–3356.

Biophysics

[36] Influence of Mg²⁺ ions on the dynamics of the guanine-sensing riboswitch

Ch. Hanke, J. Buck, H. Schwalbe, H. Gohlke

Riboswitches are genetic regulatory elements mostly located in the 5'-untranslated region of bacterial mRNA, which control gene expression upon binding of small ligand molecules with high specificity. Upon binding of the ligand to the riboswitch aptamer domain, the downstream located expression platform undergoes conformational changes and thereby influences the expression of the corresponding genes. Due to their role in gene expression, riboswitches are promising drug targets [1]. Even though several crystal structures of riboswitch aptamer domains in their bound conformation are available, structural knowledge about the unbound state of riboswitches is still scarce. Atomic-level knowledge of the unbound state will provide information about preorganization and preformation of tertiary interactions in the aptamer domain and thereby yield new information about the ligand binding process as an important step in the gene regulation by riboswitches.

The guanine-sensing riboswitch controls genes involved in the guanine metabolism and is one of the smallest and most well-studied riboswitches known. We use explicit solvent molecular dynamics (MD) simulations and replica-exchange MD simulations of the aptamer domains of the wildtype guanine-sensing riboswitch (Gsw^{apt}) and a G37A/C61U mutant (Gsw^{oop}) [2-4] at different magnesium ion concentrations to gain deeper insights into the conformational heterogeneity of the unbound state and folding pathways. Preliminary results point to a stabilizing effect of magnesium ions on the unbound aptamer domain, in agreement with experiments [2, 3].

[1] Mulhbachter, J., et al., *Therapeutic applications of ribozymes and riboswitches*. Current Opinion in Pharmacology, 2010. 10(5): p. 551-556.

[2] Noeske, J., et al., *Interplay of 'induced fit' and preorganization in the ligand induced folding of the aptamer domain of the guanine binding riboswitch*. Nucleic Acids Research, 2007. 35(2): p. 572-583.

[3] Buck, J., et al., *Dissecting the influence of Mg²⁺ on 3D architecture and ligand-binding of the guanine-sensing riboswitch aptamer domain*. Nucleic Acids Research, 2010. 38(12): p. 4143-4153.

[37] Memory consumption of neuronal network simulators at the brain scale

S. Kunkel, M. Helias, T. C. Potjans, J. M. Eppler, H. E. Plesser, M. Diesmann, A. Morrison

Simulations of neuronal networks involve the representation of numerous objects and frequent interactions between them. As this requires extensive software infrastructure, a neuronal network simulator optimized for clusters of several hundred processors can fail to run on supercomputers with of the order of 100,000 nodes due to massive serial memory overhead of insufficiently parallelized data structures. To systematically investigate this issue we developed a mathematical model of the memory usage of a neuronal network simulator. The model can be instantiated for a particular software in order to analyze the memory utilization of the constituent components for different regimes of network size and number of processes. In its original formulation the model is based on the assumption of random network connectivity, but it can be adapted to account for more structured networks, such as systems of cortical columns, which are complexes of up to 100,000 neurons with high intra-connectivity. Based on model predictions, we investigate to what extent exploiting the structure by gathering the neurons of a column on a subset of processors results in improved memory utilization.

Soft Matter Science

[38] Conformational study of stretched and unstretched semiflexible polymer chains under a good solvent condition

H.-P. Hsu, W. Paul, K. Binder

Semiflexible polymer chains under good solvent conditions are described by self-avoiding walks on the square and simple cubic lattices in $d = 2$ and $d = 3$ dimensions, respectively [1, 2], and the stiffness of chains is controlled by the bending energy ϵ_b . With the pruned-enriched Rosenbluth method (PERM), we observe a double crossover behaviour, rigid-rod-like to (almost) Gaussian random coils, then to self-avoiding walks, for the chain length up to $N = 50000$ in $d = 3$, but only a single crossover from rigid-rod-like to self-avoiding walks for the chain length up to $N = 25600$ in $d = 2$. Testing the applicability of the Kratky-Porod model, we also check whether the chain conformation is dominated by the excluded volume effects or not as the chain length and its flexibility vary. We extend our study to the problem of stretching semiflexible chains [3]. Varying the strength of the force, the flexibility of the chain, and the chain length, the theoretical predictions of the force-extension relationship at different length scale regimes (linear response - Pincus blob - Kratky-Porod model - freely joined chain) are checked. Our large scale Monte Carlo simulations give clear evidence for the importance of excluded volume effects on the stretching behaviour of semiflexible polymer chains.

[1] H.-P. Hsu, W. Paul, and K. Binder, *Europhys. Lett.* 92, 28003 (2010).

[2] H.-P. Hsu, W. Paul, and K. Binder, *Europhys. Lett.* 95, 68004 (2011).

[3] H.-P. Hsu and K. Binder, *J. Chem. Phys.* (2012) in press, e-print, arXiv:1110.1410.

[39] Adsorption of bottle brush polymers on a surface under good solvent conditions

H.-P. Hsu, W. Paul, K. Binder

The adsorption of a bottle-brush polymer end-grafted with one chain end of its backbone to a flat substrate surface is studied by Monte Carlo simulation of a coarse-grained model, that previously has been characterized in the bulk, assuming a dilute solution under good solvent conditions [1,2]. Applying the bond fluctuation model on the simple cubic lattice with the grafting density $\sigma = 1$, we vary the backbone chain length N_b and the side chain length N in the range such that they correspond well to the experimentally accessible range and theoretical scaling regime. When the adsorption energy strength ϵ is varied, we find that the adsorption transition (which becomes well-defined in the limit $N_b \rightarrow \infty$, for arbitrary finite N) roughly occurs at the same value ϵ_c as for ordinary linear chains ($N = 0$), at least within our statistical errors. Mean square end-to-end distances and gyration radii of the side chains are obtained, as well as the monomer density profile in the direction perpendicular to the adsorbing surface. We show that for longer side chains the adsorption of bottle-brushes is a two step process, the decrease of the perpendicular linear dimension of side chains with adsorption energy strength can even be non-monotonic. Also the evidence for a crossover from rod-like behaviour to the scaling of two dimensional self-avoiding walks as bottle brush polymers strongly adsorbed onto the surface is presented [3,4].

[1] H.-P. Hsu, W. Paul, and K. Binder, *Macromolecules* 43, 3094 (2010).

[2] H.-P. Hsu and W. Paul, *Comp. Phys. Comm.* 182, 2115 (2011).

[3] H.-P. Hsu, W. Paul, and K. Binder, *J. Chem. Phys.* 133, 134902 (2010).

[4] H.-P. Hsu, W. Paul, and K. Binder, *J. Phys. Chem. B* 115, 14116 (2011).

[40] Grafted and nongrafted polymer adsorption

M. Möddel, M. Bachmann, W. Janke

In the present work, we compare the thermodynamic behaviour of a finite single free polymer near an attractive substrate with that of a polymer grafted to that substrate. After we recently found first-order like signatures in the microcanonical entropy at the adsorption transition in the free case [1], and knowing that many studies on the polymer adsorption in the past have been performed for grafted polymers, the question arises, to what extent and in what way the grafting changes the natures of the adsorption transition. This question is tackled here using a coarse-grained off-lattice model and covers not only the adsorption transition, but all transitions a single polymer near an attractive substrate of varying strengths undergoes. Due to the impact of grafting especially on the translational but also on the conformational entropy of desorbed chains, the adsorption transition is affected most strongly. Our results are obtained by a combined canonical and microcanonical analysis of Monte Carlo data.

[1] M. Möddel, W. Janke, and M. Bachmann, Systematic Microcanonical Analyses of Polymer Adsorption Transitions, *Phys. Chem. Chem. Phys.* 12 11548 (2010).

[2] M. Möddel, W. Janke, and M. Bachmann, Comparison of the Adsorption Transition for Grafted and Nongrafted Polymers, *Macromolecules* 44 (22), 9013-9019 (2011).

There also exists a proceedings article concerned with this project in the current issue of the "Proceedings of the NIC Workshop 2012".

[41] Polymer Chain Inside an Attractive Sphere

H. Arkin, W. Janke

We analyze the structural behaviour of a single polymer chain inside an attractive sphere. Our model is composed of a coarse-grained polymer and an attractive sphere potential. By means of extensive multicanonical Monte Carlo simulations it is shown that the system exhibits a rich phase diagram ranging from highly ordered, compact to extended, random coil structures and from desorbed to partially or even completely adsorbed conformations. These findings are identified with different structural observables.

[42] Monte Carlo simulations of colloid-polymer mixtures in cylindrical confinement

A. Winkler, D. Wilms, P. Virnau, K. Binder

We investigate the Asakura-Oosawa model in cylindrical confinement with Monte Carlo simulations. On the one hand the system can be regarded as a model for nanopores, on the other hand the system exhibits an interesting "phase behaviour" due to its quasi-one-dimensional character. At high polymer reservoir packing fractions, the tube is either filled with liquid or gas. When we approach a "pseudo-critical point" (at reservoir packing fractions above the critical value of the bulk) several interfaces appear and the tube contains both liquid and gas phases, which are studied by extensive Free Energy calculations.

[43] Molecular Dynamic methods to locally resolve elastic quantities

E. Ricciardi, S. Butler, F. Leroy, F. Müller-Plathe

Complex multicomponent multiphase materials, generally, are composed by a polymer matrix

in which nanofillers with dimensions of few a nanometers are dispersed. When at least one of the nanomaterial constituents is composed of soft matter, the interactions between the constituents modifies the soft material microstructure in the interphase layer. It is therefore of interest to develop models able to measure and to account for possible changes in the interphase layer to predict the mechanical properties of the composite materials.

A method based on small-deformation mechanical response has been developed to locally resolve for the Poisson ratio in simple and composite materials. The method has been developed while making the assumption of periodic boundary conditions, as commonly employed in molecular simulations, and it can be directly applied to both homo- and heterogeneous systems.

A polystyrene bulk, a silica bulk, and a heterogeneous polystyrene-silica composite system have been characterized both in an unperturbed state and under imposed strain. The displacement of the atom induced by the imposed strain has been determined and, as a result, the Poisson ratio spatial profile determined. The results show the effects of the local material anisotropy present in the glassy material and in the composite system. The spatial distribution of the computed elastic quantity can be employed in micromechanical models developed to predict the overall mechanical properties of multicomponent materials, taking into account the modifications of the mechanical properties in the soft phase due to the presence of the interface.

Condensed Matter

[44] Termination of the hexagonal ice (0001)-surface by admolecule structures

A. Michl, M. Kolb, M. Bockstedte

The (0001)-surface of hexagonal ice (Ih) is conceived to be terminated by a proton-ordered bilayer [1]. For ice grown on metals, however, recent experiments report evidence that questions the bilayer-termination [2,3]. In fact, a detailed STM analysis of ice islands grown on Cu(111) demonstrated a termination by admolecule structures on top the bilayer [3]. Using density functional theory, we address the interaction of admolecules on the ice surface and analyse the observed admolecule structures. We find that admolecules coalesce into a nominal 2x1 superstructure of mutually bonded pairs. Hexagonal admolecule-rows represent low energetic structures that under compressive strain are more stable than the bilayer-termination. Their energetics much depends on the arrangement of OH-groups and the bonding of the row edge to the surface. Attachment of admolecules or admolecule pairs to the row edges yields a substantial energy gain. The latter attach either parallel or more favorably at an angle. This explains the observation of a 2x1 admolecule structure in between adjacent hexagon rows [3]. Triggered by thermal fluctuations or current injection via an STM-tip undercoordinated edge molecules may evolve to the row top into metastable positions. Our results show a trend towards an energetic stabilization of admolecule reconstructions under compressive strain.

[1] D. Pan et al., Phys. Rev. Lett. 101 (2008) 155703.

[2] Ph. Parent et al., J. Chem. Phys. 117 (2002) 10842.

[3] M. Mehlhorn and K. Morgenstern, Phys. Rev. Lett. 99 (2007) 246101.

[45] High resolution density of states in graphene with vacancies

V. Häfner, Ch. Seiler, I. Kondov, F. Evers

Disorder plays a fundamental role in transport properties of graphene. We model a specific kind of disorder, vacancies, which introduce zero modes in the density of states of graphene. The system has the peculiarity that the DOS is very sensitive at low energies to the detailed distribution of the vacancies. In this work, we treat graphene in the nearest neighbour tight-binding approximation with an equal hopping probability to all sites. Vacancies are modeled by removal of sites from the tight-binding Hamiltonian. To calculate the density of state we propagate the wave-function of the system with time using the Krylov subspace methods. This allows us to choose the spectral resolution as well as the energy range. We demonstrate the building of zero modes and a pseudo-gap for disorder in the cases of one and two sub-lattices and studied the effects of disorder concentration for models with 2048x2048 and 4096x4096 sites. The numerical results agree with the analytical formula for the BDI symmetry class derived in previous work [1].

[1] F. Evers and A. D. Mirlin, Rev. Mod. Phys. 80, 1355-1417 (2008).

[46] Dynamically induced vortex states at ferromagnetic surfaces

M. P. Magiera, D. E. Wolf

Vortex structures can occur in the two dimensional Heisenberg model, especially under a crystalline easy plane anisotropy. In this case the system behaves similar to the two

dimensional XY-model.

We show that a dipolar magnetic tip, which is magnetized perpendicular to an easy plane Heisenberg film, may induce such a vortex structure, although it would not be stable in absence of the tip. From dynamic simulations at zero temperature we show that the motion of the tip can produce or destroy vortices. If a heat bath is connected to the system, the moved tip changes the activation energy to produce a vortex-antivortex pair.

[47] Properties of geologically relevant fluids, melts and glasses from *ab initio* molecular dynamics simulations

G. Spiekermann, P. M. Kowalski, J. Dubravl, S. Jahn

Fluids and melts play an important role in many geological processes in the Earth's crust and upper mantle, such as volcanism, the chemical alteration of rocks and the formation of ore deposits. It is important to characterize the physical and chemical properties of these fluids and of dissolved species as a function of pressure, P , temperature, T , and composition, x . Experiments are usually challenging especially at extreme conditions, where measurements have to be performed *in situ*. On the other hand molecular modelling is a unique and complementary approach that allows direct access to the atomic scale structure and dynamics. First principles simulation methods that are based on density functional theory have the power to predict the molecular structure and related properties of chemically complex melts and fluids, also at extreme conditions. However, the calculations at this level of theory are computationally very demanding. The access to HPC facilities allows us to perform extensive Car-Parrinello molecular dynamics (CPMD) simulations of systems of a few hundred atoms, which is needed to study the speciation and other properties of complex fluids important for Earth science.

Here, we present three recent results of CPMD simulations performed on the BlueGene/P JUGENE. (1) We have developed a new approach to calculate the vibrational properties of silica species in MgO-SiO_2 glasses that are often investigated experimentally as simple analogs to geologically relevant melts. This is an important step to assist the experimental Raman spectroscopy band assignment for structural characterization. (2) We have developed a new method to calculate isotope fractionation between aqueous fluids and minerals. This is important to understand isotope signatures of rocks and fluids. (3) We investigate the speciation of the high field strength elements Hafnium and Zirconium in aqueous fluids at high temperatures. This complements the experimental investigations, using methods such as XANES, to explore the difference in behaviour of these two elements in solution that are often at face assumed to behave geologically very similar. Our interdisciplinary studies at the interface between theoretical physics and geochemistry make an important contribution towards the understanding and prediction of structural and chemical behaviour of geologically important materials.

[48] Non-linear single-particle-response of glassforming systems to external fields

D. Winter, P. Virnau, K. Binder, J. Horbach

Glassy dynamics of viscous liquids are characterized by a drastic slowing down of dynamical properties, while structural and thermodynamic quantities only show a weak gradual change. Recently, various independent studies have revealed that the interplay of the glass transition with external fields provides a wealth of new phenomena yet to be explored. There is hope that the understanding of the non-linear response of glassforming systems to external fields leads to new insight into the nature of the glass transition. In this work, we study the behaviour of single particles in a supercooled liquid under the influence of an external force. Our model system is a 50:50 binary mixture whose particles interact via a Yukawa potential

$$V_{\alpha\beta}(r) = \varepsilon_{\alpha\beta} d_{\alpha\beta} \exp[-\kappa(r - d_{\alpha\beta})]/r.$$

By choosing slightly different potentials between A and B particles we prevent the system from crystallizing. In the equilibrated system, we add a constant force field to one of these particles which as a consequence will be accelerated. After some time, this particle reaches a steady state. In this state we measure characteristic properties of the particle and the surrounding like the steady state velocity, the friction coefficient, mean square displacements and correlation functions in dependence of the external force and system temperature. We observe that for low temperatures and high enough force fields the particle leaves the linear response regime and enters the non-linear regime. Here, the friction coefficient is not constant any more. For even higher forces all curves reach a second plateau and fall on top of each other. This work also allows to check new theoretical approaches for the micro-rheology of glassforming systems in the framework of mode coupling theory.

Materials Science

[49] Understanding functional properties of nanostructured magnetic materials

M. E. Gruner, A. Grünebohm, P. Entel

Our work is concerned with the first principles design and understanding of modern functional materials. We concentrate on three important classes: Ultra-hard magnetic nanoparticles for data recording purposes, predicting structural stability in magnetic shape memory alloys and the stability of domain structures in ferroelectric BaTiO₃.

With the help of JUGENE we performed large-scale DFT calculations of Fe-Pt nanoclusters with up to 1415 atoms which confirm that up to diameters of about 4 nm, multiply twinned morphologies are preferred over the hard magnetic layered L1₀ structure, which is necessary for application [1].

Further investigations including spin-orbit coupling of small Fe-Pt particles decorated with organic and inorganic elements as, e.g., gold, aluminum or carbon give an account on the possible beneficial or destructive influence of a surrounding matrix and allows to derive basic design guidelines for a suitable encapsulating material [2].

Apart from the well investigated full Heusler alloy Ni₂MnGa, also disordered Fe-rich Fe-Pd alloys exhibit a sizable magnetic shape memory effect, i.e., macroscopic strains of several percent induced by magnetic field-induced shifting of martensitic twin boundaries. This effect is limited to a slightly tetragonal intermediate fct phase, which appears between the fcc austenite and bcc martensite. We demonstrate that an explicit modelling of disorder in large supercells is necessary to obtain a qualitatively correct description of the binding surface and thus a thorough understanding of the order of the structural phases [3]. This is owed to large static displacements of the atoms from their ideal lattice positions, which appear to a different extent in these phases. These arise from the different sizes of the component as well as a reconstruction of the electronic states at the Fermi level in the spirit of the Jahn-Teller effect. This leads to a low formation energy for twin interfaces and allows the formation of a nanotwinned microstructure which has been confirmed experimentally in strained epitaxial films [4].

Finally, we investigated the evolution of domain wall structures in tetragonal bulk BaTiO₃ and nanoparticles. For the bulk material, we find atomically sharp domain wall profiles for the 180° domain wall, which is not the case for the 90° domain wall. Although, we could not stabilize a ferroelectric state neither in films nor in small nanoparticles, a large local polarization exists in both cases [5].

[1] M. E. Gruner, P. Entel, *Int. J. Quant. Chem.* **112**, 277 (2012).

[2] C. Antoniak, M. E. Gruner, M. Spasova *et al.*, *Nature Communications* **2**, 528 (2011).

[3] M. E. Gruner, P. Entel, *Phys. Rev. B* **83**, 214415 (2011).

[4] S. Kauffmann-Weiss, M. E. Gruner, A. Backen *et al.*, *Phys. Rev. Lett* **107**, 206105 (2011).

[5] A. Grünebohm, M. E. Gruner, P. Entel, *Ferroelectrics*, *accepted for publication*.

[50] Amorphous Ge₁₅Te₈₅: Density functional, high-energy x-ray and neutron diffraction study

J. Kalikka, J. Akola, R. O. Jones, S. Kohara, T. Usuki

We present here a study of the amorphous structure and electronic properties of Ge₁₅Te₈₅. The study combines the results of density functional (DF) simulations and high-energy x-ray diffraction (XRD) and neutron diffraction (ND) measurements. Three different atomic models of 560 atoms have been constructed with the aid of reverse Monte Carlo method to satisfy several criterions: Good agreement with the experimental structure factors S(Q), low total

energy according to DF, and correct electronic properties (with band gap).

The models (a) and (c) are based on a DF structure (simulated annealing), which was produced by heating an amorphous sample up to viscous regime at 500K and cooled down in 5 subsequent simulations at 500, 450, 400, 350 and 300K for 20 ps each. The structure was then optimized. The model (b) is based on an RMC-based structure that was optimized with DF. The RMC refinement of these structures consists of short RMC-runs that produce structures 100 ± 5 meV/atom above the annealed structure in DF potential energy while improving the agreement with experimental data. Models (a) and (b) use equal fitting weights for XRD and ND datasets without Ge-Ge bonds, while the model (c) uses higher weight on ND with Ge-Ge bonds.

The structure which had a small number of Ge-Ge bonds was the one that reconciled best with the different criterions: The agreement of $S(Q)$ is good for *both* XRD and ND and the electronic structure shows a small band gap at the Fermi energy (semiconductor). This finding suggests that Ge-Ge bonds, albeit their small number, should not be excluded from the amorphous structure.

Ge coordination displays an interesting co-existence between tetrahedral fourfold coordination and defective octahedral 3+3 coordination as observed for the GeTe and $\text{Ge}_2\text{Sb}_2\text{Te}_5$ alloys previously, and both situations are equally likely to occur. The obtained bond orders confirm that there is a difference in chemical bonding between the two types of Ge and illustrate the variation of bond strength as a function of distance. The Ge-Te and Te-Te bonds are nearly-covalent, and a reasonable cutoff distance for counting bonds lies around 3.0-3.2 Å for this class of chalcogenide materials.

[51] *Ab initio* calculations on van der Waals interactions in defective graphene

M. Hassan, M. Walter, M. Moseler

A study of the interaction of the benzene molecule with several graphene-based structures has been conducted. This study was motivated by the question how polymers containing phenyl groups (e.g. polystyrol) interact with reduced GO. We have considered 24 structures representing pristine graphene and some of its most common defects, include topological defects, vacancies and functional groups. Within the density functional theory, two different state of the art computational approaches to calculate vdW interactions are considered. The two approaches agree well qualitatively, but show a systematic quantitative deviation. Adsorption of benzene on defective graphene is not very different to adsorption on pristine graphene. For most of the defects considered, at most 25% of the interaction energy has been lost. Among the four most stable structures (more stable even than benzene on pristine graphene) in our study, two include an oxygen atom replacing an carbon atom in the graphene sheet, one is a topological defect and one represents a negatively-curved graphene sheet emerging after functional group attachment. The five least stable structures exclusively contain epoxy / hydroxyl groups where geometrical considerations force the adsorbed molecules be further away from the substrate. We have extended the investigation to interaction of benzene with strained graphene. Stretching of graphene along three different directions [zigzag, armchair, both], resulted in a linear proportionality between the adhesion energy and the substrate "filling factor" defined as the number of atoms per square angstroms. The linearity parameters are independent of our choice for the direction of the strain and suggest that the effect is mainly geometrical. This trend should be relevant for experiments and applications that involve mechanical stress tests.

[52] DFT study on the oxidative dehydrogenation of methanol on ceria supported vanadia catalysts: First steps

J. Paier, Ch. Penschke, J. Sauer

The selective oxidation of methanol to formaldehyde has been widely studied with vanadium-oxide catalysts (e.g. [1]). The reaction is believed to follow a Mars-van Krevelen mechanism, in which the water produced in the overall reaction is formed using lattice oxygen from the solid surface. Moreover, it is well known that the effect of the support (e.g. ceria, titania etc.) on the catalyst's activity can be dramatic, but a detailed understanding is still missing. Doubtlessly, accurate theoretical calculations represent a valuable route towards a more complete picture (e.g. [2]).

The first phase of this work focuses on the accuracy of state-of-the-art density functional-based methods (DFT+U, hybrids). These approaches are able to deal with so-called narrow band, localized electrons ubiquitous in the reduced, i.e. O-defective catalyst, contrary to standard semilocal functionals. Calculated structural properties and formation energies of complex vanadia, ceria and titania bulk- and surface phases, including careful estimates of vibrational effects as well as the dispersion energy contribution are presented. These results allow for a critical assessment of the underlying methodology via comparisons with experiment giving valuable error margins needed for estimates on thermochemical properties, such as reaction energies or barrier heights [3,4].

[1] B.M. Weckhuysen, D.E. Keller, *Catal. Today* 78, 25 (2003).

[2] M.V. Ganduglia-Pirovano, C. Popa, J. Sauer, H. Abbott, A. Uhl, M. Baron, D. Stacchiola, O. Bondarchuk, S. Shaikhutdinov, H.J. Freund, *J. Am. Chem. Soc.* 132, 2345 (2010).

[3] J. Sauer, J. Döbler, *Dalton Trans.* 19, 3116 (2004).

[4] X. Rozanska, R. Fortrie, J. Sauer, *J. Phys. Chem. C* 111,6041 (2007).

[53] Computational studies of Si nanocrystals embedded in an amorphous SiO₂ matrix

K. Seino, F. Bechstedt

Properties of silicon nanocrystals have been experimentally and theoretically widely studied due to their potential for Si-based optoelectronic, memory devices and next generation solar cells. One of the most striking and best studied effects in semiconductor nanocrystals is the quantum size effect — an inverse correlation between the optical gap and the nanocrystal size. Effects due to spatial quantization promise to overcome the limitations of the indirect-gap semiconductors for optoelectronic applications. Even optical gain has been achieved in Si nanocrystals [1]. However, a complete understanding of the origin and the mechanism of the luminescence is still missing. The Si nanocrystal properties appear to be very sensitive to their Si/SiO₂ interface and their size distribution. Although there are many experimental studies on Si nanocrystals embedded in an amorphous SiO₂ matrix, there are fewer calculations on embedded Si nanocrystals because of the large computational efforts. Usually the theoretical investigations are performed on simpler model systems, e.g. hydrogenated Si nanocrystals. Here we present results of large-scale calculations for Si nanocrystals embedded in silica glass based on density functional theory [2, 3]. In our simulations realistic Si nanocrystals with diameters ranging between 0.8 and 1.6 nm, i.e., up to systems with more than 1000 atoms, are treated. We demonstrate the influence of the interface between nanocrystal and matrix on the electronic and optical properties in order to compare with isolated hydrogenated Si nanocrystals. Moreover, we compute the spatial variation of the electronic structure for embedded Si nanocrystals and discuss interfacial electronic properties such as local band gaps and band offsets.

[1] L. Pavesi, L. Dal Negro, C. Mazzoleni, G. Franzò, and F. Priolo, *Nature* 408, 404, 2000.

[2] K. Seino, F. Bechstedt and P. Kroll, Nanotechnology 20, 135702, 2009.

[3] K. Seino, F. Bechstedt and P. Kroll, Phys. Rev. B 82, 085320, 2010.

[54] KKRnano: Precise density functional calculations for thousands of atoms

A. Thiess, R. Zeller, M. Bolten, E. Rabel, P. H. Dederichs, St. Blügel

KKRnano is a newly developed large-scale electronic structure code applicable to insulating, semiconducting and metallic materials. The challenge to deal with many thousands of atoms per supercell within a first principles description is mastered by massively parallelizing the code for use of up to hundred thousand processors. We will describe how high computational and parallel efficiency can be reached by introducing e.g. a preconditioned iterative solution of the Dyson equation. Beyond the introduction to the methodology we will present an application to the phase change material GeSbTe - a material in which disorder treated within large-scale supercells plays a central role.

Computer Science

[55] Supercomputer modeling of locally resolved processes in DMFC stacks

J. McIntyre, A. A. Kulikovsky, D. Stolten

A highly scalable quasi-3D model of a large 1-kW class DMFC stack is developed. The model takes into account heat and current transport in the bipolar plates, coupled to the through-plane transport in the membrane-electrode assemblies. The electrochemical model is an extension of a Perry-Newman-Cairns model with the Butler-Volmer rate of electrochemical conversion [1]. A quasi-two phase model is used to describe the anodic flow, and a simple modelling parameter, k , is introduced to describe the acceleration of the flow rate due to CO₂ bubbles [2].

The stack is subdivided into a large number of elementary geometrical units. Each unit has an associated numerical mesh for each significant variable. Spatially these meshes correlate to the bipolar plates within the DMFC stack. The model is intended to run using supercomputing resources, and so each subdivided unit is solved on a separate processor, thus allowing a high degree of flexibility and scalability regarding stack dimensions, and available computing power.

The model is used to simulate the regimes with differing methanol flow. In each case the middle cell in a 5-cell stack is considered. The cell is divided into two halves of equal area, and supplied with two different feed velocities. Additionally, simulations were also done for broader differences across the entire stack, whereby each cell in the stack was fed with the same differing feed regime.

The results show that the local current in the lower feed region has a more moderate gradient, while in the current increases in the higher feed region to compensate for this drop. By coupling the two regions together, a smoothing of the current distribution is achieved. A compensation effect is visible in the current profiles. The $\lambda = 4$ side produces current above that of the reference, and the $\lambda = 1.2$ exhibits a much gentler fall-off than in the reference case.

[1] A. Kulikovsky, *Journal of The Electrochemical Society*, 152 (2005), A1121-A1127.

[2] A. A. Kulikovsky, *Electrochemistry Communications* 51 (2005) 237-243.

Simulation Laboratories at Jülich Supercomputing Centre

For some years now there has been a growing realisation that application software is lagging behind HPC hardware developments. While several Petaflop-scale supercomputers are now available worldwide, it is becoming increasingly difficult to exploit these machines with single applications. Substantial efforts are needed in order to enable computational science communities to solve problems with high scientific impact through efficient use of high-end supercomputing resources.

To help meet this challenge the Jülich Supercomputing Centre (JSC) has proposed a new type of domain-specific research and support structure: the Simulation Laboratory (SimLab). Initially four such units have now been established at JSC in the fields of Computational Biology, Climate Science, Molecular Systems and Plasma Physics, which have already been actively engaged with user groups from their respective communities over the past years. Last year three additional SimLabs have been created: *Ab Initio*, Fluid & Solid Engineering, Nuclear & Particle Physics.

[56] SimLab Biology

J. Meinke, S. Mohanty, O. Zimmermann

The SimLab Biology supports and performs research in computational biology ranging from *de novo* assembly of next-generation sequencing data to protein folding simulations. Our goal is to make the computational resources at the Jülich Supercomputing Centre accessible to biologists.

To achieve this goal we provide, evaluate, and develop software that takes advantage of large parallel computers and accelerators such as GPUs. We investigate new algorithms that are highly scalable. Our range of expertise covers, e.g., molecular dynamics, Monte Carlo, and machine learning. We co-develop two high-performance Monte Carlo protein simulation codes (ProFASi and SMMP) and apply them to important biological questions. Finally, the SimLab Biology provides advice, training, and support to life scientists that want to use supercomputers to tackle new problems in computational biology.

[57] SimLab Climate Science

S. Griessbach, L. Hoffmann, C. Hoppe

The SimLab Climate Science (SLCS) in the Jülich Supercomputing Centre was established in 2010. The SLCS provides support and carries out own research projects in atmospheric research and climate modelling.

The topics covered by the SLCS are inverse modelling, remote sensing of trace gases, aerosols and clouds, data assimilation, and modelling of atmospheric chemistry and dynamics. Team members are experienced with the Jülich RAPid Spectral Simulation Code (JURASSIC), the Chemical Lagrangian Model of the Stratosphere (CLaMS), the ECMWF Hamburg (ECHAM)/Modular Earth Submodel System (MESSy), Weather Research and Forecasting (WRF), and the Community Earth System Model (CESM). The research highlights presented here are gravity wave and deep convection detection from Atmospheric InfraRed Sounder (AIRS) data, volcanic ash detections from Michelson Interferometer for Passive Atmospheric Sounding (Envisat MIPAS) data and stratospheric water vapor simulations with a coupled CLaMS-ECHAM/MESSy model.

[58] SimLab Molecular Systems

V. Chihai, R. Halver, Th. Müller, A. Schiller, G. Sutmann

The SimLab Molecular Systems was founded at JSC to support projects in the field of *ab initio* quantum chemistry, atomistic force field and coarse grain simulations. Main focus is given to the analysis and improvement of scalability and runtime behaviour of codes in order to enable an efficient parallel execution. Also the co-development of methods and algorithms is supported. Simulation codes like Columbus, Turbomole or MP2C are actively supported and developed. In addition members of the simulation laboratory are active partners in various national and international projects, including exascale projects like Mont Blanc or EESI.

[59] SimLab Plasma Physics

L. Arnold, D. Brömmel, P. Gibbon, C. Hövel, A. Karmakar, M. Winkel

The SimLab Plasma Physics (SLPP) is a research and support group with expertise in advanced simulation techniques needed for tackling the highly nonlinear, multi-dimensional problems prevalent in contemporary plasma theory. One of its main tasks is to actively engage with national and European plasma groups, helping them to harness the world-class supercomputer facilities available at JSC.

The expertise of the SLPP covers pure mesh based methods, mainly used in magneto hydrodynamics, particle-mesh methods, like particle-in-cell, as well as pure particle methods. At the field of mesh-free methods, SLPP provides a highly scalable tree code (PEPC) to compute n-body interactions. This code is developed at JSC and is used in multiple scientific areas. Beside PEPC, we provide high level support for various plasma-physical codes. The past support activities included the scalability of the implementations of methods like particle-in-cell and multi-grid. In the latter case SLPP enabled the code to scale on up to 128k cores of IBM Blue Gene/P. Our exascale activities include the participation in projects like TEXT, Mont Blanc or EIC.

[60] JARA-HPC SimLab *Ab Initio*

E. Di Napoli

In condensed matter physics and quantum chemistry, *ab initio* simulations are becoming the standard method for investigating properties of materials. JARA-HPC SimLab *Ab Initio* (SLAI) is beginning to establish a user-friendly environment for the development of new methods to be used in the vast realm of materials science simulations. The Lab will be responsible for identifying current research directions in the field of high-performance computing and make them visible to the community at large.

By analyzing cutting edge simulations, SLAI aims to show evidence of the need of developing new methods. The focus is on conducting thorough analysis of material simulations with the purpose of extracting information to be used for advancing the *ab initio* computational paradigm. The objective is to apply a novel concept that integrates knowledge from simulations into the structure of the computational paradigm to enable the simulation of new physics. It is then natural that the team of the Lab will closely collaborate with the cross-sectional groups Immersive Visualization, Parallel Efficiency, and Numerical Algorithms.

Research conducted at the Lab will illustrate that is possible to use numerical and analytical techniques to enhance computational methods used in *ab initio* simulations. Once running at

full speed, SLAI will have established a methodology centered around analysis of simulations, performance optimization, and parallelization of algorithms, to be used in support of current and future physics-oriented simulations.

Participants

Name	First Name	Affiliation	City	Poster No.
Abma	Dick	MPI-Meteorologie	Hamburg	
Ansorge	Cedrick	Max Planck Institute for Meteorology	Hamburg	
Arnold	Lukas	Forschungszentrum Jülich	Jülich	59
Athenodorou	Andreas	DESY Zeuthen	Berlin	
Atodiresei	Nicolae	Forschungszentrum Jülich	Jülich	
Bachem	Achim	Forschungszentrum Jülich	Jülich	
Banerjee	Robi	Universität Hamburg	Hamburg	
Bauer	Dieter	University of Rostock	Rostock	
Behr	Marek	RWTH Aachen University, JARA-HPC	Aachen	
Biermann	Peter	Max-Planck-Institute for Radioastronomy	Bonn	
Binder	Kurt	Johannes Gutenberg Universität Mainz	Mainz	
Bischoff-Gauß	Inge	Karlsruher Institut für Technologie	Karlsruhe	30
Bockstedte	Michel	FAU Erlangen-Nürnberg	Erlangen	44
Bourdin	Philippe-A.	Kiepenheuer-Institut für Sonnenphysik	Freiburg	13
Brehm	Martin	Universität Leipzig	Leipzig	33
Breslau	Andreas	Max-Planck-Institut für Radioastronomie	Bonn	19
Böckmann	Rainer	Universität Erlangen-Nürnberg	Erlangen	
Denev	Jordan A.	Karlsruhe Institute of Technology	Karlsruhe	
Di Napoli	Edoardo	Forschungszentrum Jülich	Jülich	60
Diesmann	Markus	Forschungszentrum Jülich	Jülich	
Dietze	Georg	RWTH Aachen	Aachen	29
Dopieralski	Przemyslaw	Ruhr-Universität Bochum	Bochum	
Doychev	Todor	KIT	Karlsruhe	28
Dürr	Stephan	Forschungszentrum Jülich & Universität Wuppertal	Jülich / Wuppertal	2
Eppler	Jochen Martin	Forschungszentrum Jülich	Jülich	
Fedosov	Dmitry A.	Forschungszentrum Jülich	Jülich	
Flynn	Jonathan	University of Southampton	Southampton	1
Foyi	Holger	Universität Siegen	Siegen	20
Gauding	Michael	RWTH Aachen	Aachen	22
Geiser	Georg	RWTH Aachen	Aachen	
Gmeiner	Björn	Universität Erlangen-Nürnberg	Erlangen	
Gottstein	Günter	RWTH Aachen University	Aachen	
Grieshammer	Steffen	RWTH Aachen	Aachen	
Grießbach	Sabine	Forschungszentrum Jülich	Jülich	57
Grope	Benjamin	RWTH Aachen	Aachen	
Groß	Axel	Universität Ulm	Ulm	

Name	First Name	Affiliation	City	Poster No.
Gruner	Markus	Universität Duisburg-Essen	Duisburg	49
Göbbert	Jens Henrik	RWTH Aachen University	Aachen	23
Halver	Rene	Forschungszentrum Jülich	Jülich	
Hanke	Christian	Heinrich-Heine-Universität	Düsseldorf	36
Hanke	Florian	Max-Planck-Institut für Astrophysik	Garching	7
Harlacher	Daniel	GRS	Aachen	25
Harting	Jens	University of Stuttgart	Stuttgart	
Hassan	Mohamed	University of Freiburg	Freiburg	51
Helias	Moritz	Forschungszentrum Jülich	Jülich	
Hennig	Fabian	RWTH Aachen University	Aachen	
Holewa	Axel	DLR	Berlin	24
Homberg	Willi	Forschungszentrum Jülich	Jülich	
Horbach	Jürgen	Heinrich Heine-Universität	Düsseldorf	
Hossfeld	Friedel	Forschungszentrum Jülich	Jülich	
Hsu	Hsiao-Ping	Johannes Gutenberg Universität Mainz	Mainz	38, 39
Janke	Wolfhard	Universität Leipzig	Leipzig	41
Jones	Robert	Forschungszentrum Jülich	Jülich	
Kaczmarek	Thomas	Max-Planck Institut für Radioastronomie	Bonn	8
Kalikka	Janne	Forschungszentrum Jülich	Jülich	50
Kalthoff	Norbert	Karlsruher Institut für Technologie	Karlsruhe	
Kamps	Martina	Forschungszentrum Jülich	Jülich	
Karsch	Frithjof	Universität Bielefeld	Bielefeld	
Koenders	Christoph	TU Braunschweig	Braunschweig	15
Kondov	Ivan	Karlsruhe Institute of Technology	Eggenstein-Leopoldshafen	45
Kremer	Manfred	Forschungszentrum Jülich	Jülich	
Kumbhar	Pramod	Forschungszentrum Jülich	Jülich	
Kunkel	Susanne	Albert-Ludwig University of Freiburg	Freiburg i. Br.	37
Kurth	Thorsten	Bergische Universität Wuppertal	Wuppertal	4
Kurtz	Wolfgang	Forschungszentrum Jülich	Jülich	31
Körfggen	Bernd	Forschungszentrum Jülich	Jülich	
Köttgen	Julius	RWTH Aachen	Aachen	
Lippert	Thomas	Forschungszentrum Jülich	Jülich	
Liseykina	Tatyana	Universität Rostock	Rostock	
Lücke	Monika	GRS	Aachen	
Magiera	Martin	Universität Duisburg-Essen	Duisburg	46
McIntyre	John	Forschungszentrum Jülich	Jülich	55
Mehrling	Timon	Universität Hamburg / DESY	Hamburg	17
Meinke	Jan	Forschungszentrum Jülich	Jülich	56
Meißner	Ulf-G.	Univ. Bonn & Forschungszentrum Jülich	Bonn	

Name	First Name	Affiliation	City	Poster No.
Mellado	Juan Pedro	Max Planck Institute for Meteorology	Hamburg	9
Miranda Mena	Joaquin G.	GRS	Jülich	
Mnich	Joachim	DESY	Hamburg	
Muramatsu	Alejandro	Universität Stuttgart	Stuttgart	
Möddel	Monika	Universität Leipzig	Leipzig	40
Müller	Claus Axel	Gauss Centre for Supercomputing e.V.	Bonn	
Müller	Marcus	Georg-August-Universität	Göttingen	
Müller	Thomas	Forschungszentrum Jülich	Jülich	
Münster	Gernot	Westfälische Wilhelms-Universität Münster	Münster	
Müser	Martin	Forschungszentrum Jülich	Jülich	
Nadler	Walter	Forschungszentrum Jülich	Jülich	
Nägel	Arne	Goethe-Universität	Frankfurt/Main	21
Paier	Joachim	Humboldt-Universität zu Berlin	Berlin	52
Paul	Wolfgang	Martin Luther Universität	Halle	
Peters	David	RWTH Aachen University	Aachen	
Pfalzner	Susanne	Max-Planck-Institut für Radioastronomie	Bonn	
Pleiter	Dirk	Forschungszentrum Jülich	Jülich	
Plesa	Ana-Catalina	German Aerospace Center (DLR)	Berlin	14
Popov	Alexey	Leibniz-Institute for Solid State and Materials Research	Dresden	34
Pérez Rubio	Paula	Universität Regensburg	Regensburg	3
Raettig	Natalie	Max-Planck-Institut für Astronomie	Heidelberg	12
Riccardi	Enrico	TU Darmstadt	Darmstadt	43
Rohlfs	Wilko	RWTH Aachen University	Aachen	29
Rushchanskii	Konstantin	Forschungszentrum Jülich	Jülich	
Saini	Jagmohan	Heinrich-Heine University	Düsseldorf	35
Schiel	Rainer	University of Regensburg	Regensburg	6
Schierholz	Gerrit	DESY	Hamburg	
Schiller	Annika	Forschungszentrum Jülich	Jülich	
Schlottke	Michael	RWTH Aachen/JARA-HPC	Aachen	
Schlößer	Tobias	Forschungszentrum Jülich	Jülich	
Schumacher	Jörg	TU Ilmenau	Ilmenau	26
Seino	Kaori	Friedrich-Schiller-Universität Jena	Jena	53
Seitenzahl	Ivo	Max-Planck-Institute for Astrophysics	Garching	10
Selke	Walter	RWTH Aachen	Aachen	
Siegert	Gabriele		Duisburg	
Sommer	Rainer	DESY	Zeuthen	
Sperling	Philipp	Universität Rostock	Rostock	18
Spiekermann	Georg	GFZ Potsdam	Potsdam	47
Spörkel	Lasse	RWTH Aachen	Aachen	

Name	First Name	Affiliation	City	Poster No.
Steinhausen	Manuel	Max-Planck-Institut für Radioastronomie	Bonn	11
Sutmann	Godehard	Forschungszentrum Jülich	Jülich	58
Szabo	Kalman	Bergische Universität Wuppertal	Wuppertal	5
Truhetz	Heimo	University of Graz	Graz	32
Vernisse	Yoann	TU Braunschweig	Braunschweig	16
Wessel	Stefan	RWTH Aachen	Aachen	
Winkler	Alexander	Johannes Gutenberg-Universität	Mainz	42
Winter	David	Johannes Gutenberg-University	Mainz	48
Wittig	Hartmut	University of Mainz & Helmholtz Institute Mainz	Mainz	
Wolf	Dietrich	Universität Duisburg-Essen	Duisburg	
Zeller	Rudolf	Forschungszentrum Jülich	Jülich	54
Zeng	Peng	RWTH Aachen University	Aachen	27
Zinn-Justin	Jean	CEA	Gif-sur-Yvette Cedex	

This list has been drawn up for the participant's personal information. It may not be passed on to third parties or used for any other purpose.